Hindawi Publishing Corporation
Advances in Optics
Volume 2014, Article ID 891395, 24 pages
http://dx.doi.org/10.1155/2014/891395

Review Article

Hybrid Materials for Integrated Photonics

Paolo Bettotti

Nanoscience Laboratory, Department of Physics, University of Trento, Via Sommarive 14, Povo, 38123 Trento, Italy

Correspondence should be addressed to Paolo Bettotti; paolo.bettotti@unitn.it

Received 5 January 2014; Revised 21 March 2014; Accepted 24 March 2014; Published 26 June 2014

Academic Editor: Shouyuan Shi

In this review materials and technologies of the hybrid approach to integrated photonics (IP) are addressed. IP is nowadays a mature technology and is the most promising candidate to overcome the main limitations that electronics is facing due to the extreme level of integration it has achieved. IP will be based on silicon photonics in order to exploit the CMOS compatibility and the large infrastructures already available for the fabrication of devices. But silicon has severe limits especially concerning the development of active photonics: its low efficiency in photons emission and the limited capability to be used as modulator require finding suitable materials able to fulfill these fundamental tasks. Furthermore there is the need to define standardized processes to render these materials compatible with the CMOS process and to fully exploit their capabilities. This review describes the most promising materials and technological approaches that are either currently implemented or may be used in the coming future to develop next generations of hybrid IP devices.

1. Introduction

Photonics is a pervasive technology with a widespread number of technological applications [1]. All around us we are surrounded by photonic devices: from the monitor you are probably using to read this paper to the fluorescent (or LED) lamp that illuminates the room you are sitting in.

Nowadays photonics is the leading technology in broadband long range communication systems and is the only foreseen solution to support the exponential increase of Internet traffic in the coming years [2]. For short link lengths and smaller bandwidths, electronic systems are still more efficient than the photonic paradigm [3] but Integrated Photonics (IP) is steadily pushing the limit where photonics becomes competitive with electronics to shorter and shorter distances as demonstrated by the commercialization of the first all-optical links for board to board connections. Both Corning and Sumitomo released optical cables compatible with the Thunderbolt technology that achieve the impressive bandwidth of 10 Gb/s. These cables use optoelectronic interfaces to convert electrical into optical signals and vice versa and are fully transparent for the end user. It is expected that, in the near future, similar standard will be available for intraboard and chip to chip systems.

Ideally photonics is a much more efficient platform to develop communication systems: photons do not interact with each other in linear regime; they do not dissipate heat along the transmission line and logical operation may be performed at much higher speed using optics rather than electronics. Thus a single optical cable transmits several independent streams of bits at tens of Gb/s of modulation rate without the need for thermal dissipation system. The different streams of bits are separated at the output port without the need for deconvolution processes (such as Fourier transforms). Furthermore in the last years scientific community started to recognize the potential of photonics to achieve parallel (vectorial) computation [4–7] and to define logical paradigms beyond the binary one, able to perform complex function within a single operation [8, 9].

Despite these intriguing possibilities, statistics tell us that the amount of energy required to sustain the increasing demand of Internet services is exponentially growing. Thus in order to become a viable alternative to electronics, photonics needs to greatly improve the efficiency of data handling. Recent studies estimate that the power consumed by Internet data center accounts for few percents of the total power produced in developed countries and that these numbers will grow in the future driven by the large numbers of services

available (e.g., cloud and virtualization applications) [10–12]. Compared to electronics the main limitation of photonics relies on its intrinsic reduced scalability. In fact the typical length scales of electrons and photons differ by orders of magnitude (Ångstrom versus hundreds of nm), and this reflects on the level of integration achievable in electronics and photonics, respectively. Thus the need of a higher level of integration and the development of integrated photonics (IP) is of primary importance in order to fully exploit the potential given by the use of light in both communication and computing systems.

IP is an active research field since 80s (reviews about the history of integrated photonics can be found in [13, 14]) and its advances are tightly bound to the evolution of the complementary metal oxide (CMOS) platform and nano-/microelectronic processes. In fact IP is often based on semiconductor technology (such as lithography and etching) and it exploits many technologies used in micro- and nanoelectronics. Unlike the electronics counterpart, photonics is based on a greater number of elementary building blocks. Such flexibility, in turns, is exploited to design and realize components with highly tailorable properties. On the other hand the large number of materials and fabrication processes involved induced fragmentation of the fabrication technologies and a lack of standard that, in the end, have slowed down the development of a common technological platform that may be used to implement those elementary building blocks.

Among the different materials used in photonics, inorganic semiconductors play a major role. Their chemical, mechanical, and thermal stability facilitates technological fabrication processes. Furthermore the integration of any functional building block (e.g., photonic) within an electronic device requires being compatible with the ubiquitous CMOS paradigm. In turn this means that strict constraints have to be fulfilled in terms of materials and process layout to exploit the CMOS technological platform.

In nearly all the main applications' fields described above silicon is a leading material to develop and fabricate photonic devices: optical fibers are typically made of silicon dioxide and exploit the low polarizability of the atomic bonds to reduce absorption in the telecommunications spectral windows (which roughly cover the range between 0.8 and 1.6 μm). Polymers based fibers, on the other hand, suffer from relatively large absorption in the near infrared and they would require periodic regeneration/amplification of the signal in long distance communication systems.

Furthermore to fully exploit the possibilities given by the photonics, photons have to be effectively confined within small volumes. In this way the strength of the light matter interactions is increased and it can be exploited to enhance both linear and nonlinear effects and to realize high efficient devices. Thus, generally speaking, a high level of integration in photonics requires the use of materials with high refractive index because the confinement of light is more effective in materials with high dielectric constant.

But despite the prevalence of the "*high index*" and the CMOS paradigms, the use of organic materials in silicon-based photonic devices enables the implementation of novel and more complex functionalities that are otherwise extremely difficult (if not impossible) to achieve using a fully inorganic approach.

If we consider the applications of hybrid photonics in information and communication technology (ICT), slot waveguides (WGs) filled with polymeric materials are studied to realize fast electrooptical modulators, while the use of polymeric cladding on top of silicon microresonators allows for fine compensation of the drift due to thermal effect in optical microresonators and the fabrication of athermal optical switches. This achievement is of great importance to reduce the energy consumption due to active trimming of the microcavities and to precisely tune the resonant wavelength using a passive mechanism.

Organic based photonics will never rival the inorganic counterpart in ICT applications, mainly because of material limits in terms of stability and transparency. Nevertheless there are several niche markets where CMOS technology shows its limits (from automotive to RF technology to personalized medicine), in which organic and hybrid photonics may play an important role. Among the others two important examples are biodegradable (implantable) sensors [15, 16] and flexible (wearable) optoelectronic [17, 18] devices. Here hybrid systems may be used to fabricate wearable sensors and advanced sensing interfaces for continuous health monitoring.

Furthermore plastics based devices are often cheaper and lightweight, can be manufactured with simplified processes (such as printing, hot embossing, and roll-to-roll [19–22]), and, in the end, have a reduced environmental footprint.

Here is a note about the term "*hybrid*." It has different meanings depending on the scientific background of the scientist that uses it: for chemists and physics and material scientists hybrid materials are materials whose components are intimately mixed at the atomic/molecular scale. A typical example is the sol-gel method that uses molecular precursors to obtain bulk glass with well-controlled structure, composition, and properties. On the other hand, from an engineering point of view, the term "*hybrid photonics*" has a different meaning. In fact, because of the ubiquity of silicon in fabrication technologies, the term hybrid describes the integration of materials that are not compatible with the standard CMOS technology. In particular the hybrid approach to photonics considers the integration of efficient light sources made of III/V or II/VI semiconductors onto a silicon-based photonic circuit. The development of such a hybrid technology raised a very large interest from both research and industrial point of views in the last years when it became evident that silicon-based light source will not be available within a short timescale and that active photonics will require the integration of efficient light sources made of other types of elements. Figure 1 describes the main classes of materials considered in this review and the type of relations among them to define the hybrid photonic topic. Polymers and III/V materials are usually coupled with a silicon photonic layer and they are used to add functionalities to the optical circuit that are otherwise difficult to implement. As mentioned above hybrid materials are often not directly compatible with the standard CMOS technology: several heavy elements are considered as contaminant in CMOS

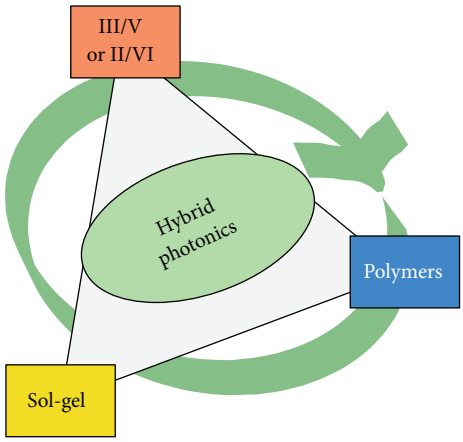

Figure 1: Schematic of the classes of materials described within this review and of their relations with defining the hybrid photonics topic.

foundry's clean environment and cannot be handled and processed together with semiconductors. Thus III/V and II/VI materials are typically integrated in a back-end process. But despite these limitations the number of integrated devices within the hybrid silicon technology is growing at a fast pace [23]. On the other hand organic materials require a careful choice of the process steps because of their weak resistance to mechanical and thermal stresses. Thus the fabrication of hybrid photonics that integrates both organic and inorganic materials is challenging from a technological point of view because it requires the modification of the standard fabrication steps in order to integrate CMOS technology with those foreign materials. Furthermore this approach cannot be easily standardized because of the large choice of potential materials that may be used and the different implementation they require. Thus innovations in this field are often hampered by technological compatibility issues, rather than by their own real performance limits.

The topic treated in this paper is extremely broad and cannot be exhausted in a single review. The arguments treated here are those considered as most promising and likely to be converted into real devices in a medium time period.

Section 1 motivates the need for deeper integration among the silicon photonic platform and classes of functional materials that despite not being considered as compatible CMOS may greatly increase the functionalities of photonics devices. Section 2 discusses the most important compound semiconductor materials and how they are used to add specific functionalities to the silicon-based optical circuit. Section 3 describes how III/V and II/VI materials are integrated on top of a silicon-based photonics layer. This hybrid integration overcomes many of the limits of silicon platform and permits the realization of efficient active photonic devices. Section 4 describes the recent advances in the fabrication of optoelectronic systems created by integrating graphene layers on top of the silicon-based optoelectronic platform. Section 5 gives an overview over the recent achievements of the integration of functional polymers with the silicon photonics and also discusses key elements organic light emitting devices. The sol-gel method is briefly discussed in Section 6 with regard to its potential and its main limits in the realization of integrated devices.

2. III/V Materials for Hybrid Photonic Devices

2.1. Hybrid III/V Light Emitting Devices. It is nowadays well known that the achievement of stimulated emission in silicon still remains a huge challenge due to the indirect band gap of the material and the consequent nonefficient optical transitions. To create light emitting devices, scientists considered the use of direct band gap materials, like III/V material (like GaAs and InP), where the two-particle process allows for a fast radiative recombination, in which both lowest energy points of valence band and conduction band share the same crystal momentum [24]. Despite these intrinsic limits, silicon will remain the leading material for integrated photonics for the next decades, driven by its compatibility with the CMOS platform.

Concerning the design of hybrid light emitting cavity, two main geometries are generally considered and they are both based on an evanescent coupling scheme [25]. The first one confines the optical mode emitted by III/V multiple quantum well structure within the underlying Si waveguide [26]. A scheme of this configuration is represented in Figure 2(a). By changing the waveguide width and the coupling strength between the active material and the silicon optical circuit, we can drastically change the confinement of the optical mode inside the waveguide and so tune the devices behavior to realize either laser or amplifiers with different quantum well confinement factor.

The other configuration that can be used consists in structuring the III/V material with microresonator geometry. In this case the optical mode is completely confined inside this III/V semiconductor layer [27], as described in Figure 2(b). The coupling with the silicon waveguide is based on the intracavity evanescent coupling scheme. This design is able to reduce the dimension of the device to about ten microns and thus allows the fabrication of highly integrable ultrasmall microrings laser on a single Si-based wafer. By combining the use of such design with cavities tuned at different resonant wavelength, it is also possible to create wavelength division multiplexing source devices on the same chip, as demonstrated by [28].

One of the most critical points of such structures remains the coupling of the optical mode between the III/V structure and the silicon waveguide, especially in the second case where the optical mode is strongly confined in the III/V material, which requires a thin layer between the two structures. Recently, Lamponi et al. in [29] and Keyvaninia et al. in [30] reported some intracavity double taper structure, using taper-based mode transformers in both the III/V and silicon waveguides, which provide high efficiency and large optical bandwidth coupling. A design of such structure is represented in Figure 3. In this last article, by thermally tuning the silicon ring resonator with NiCr deposition above it, the authors also demonstrated the tunability of the emission wavelength of their single mode laser with a 10 nm wavelength span range.

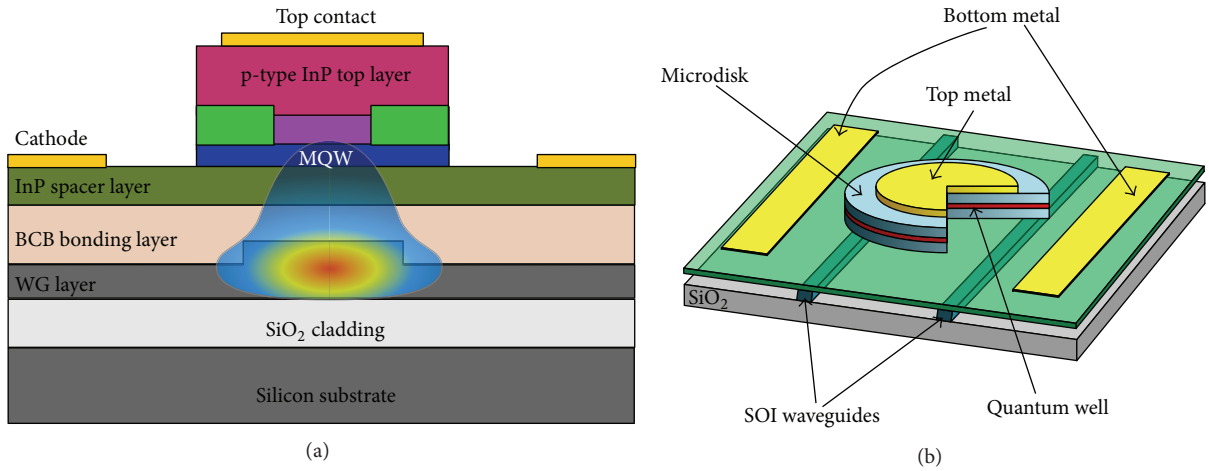

FIGURE 2: Two examples of hybrid integration of III/V active materials on top of a silicon-based photonic layer: (a) a multiple quantum well cavity evanescent coupled to an underlying silicon waveguide; (b) a III/V microresonator evanescent coupled to Si WGs.

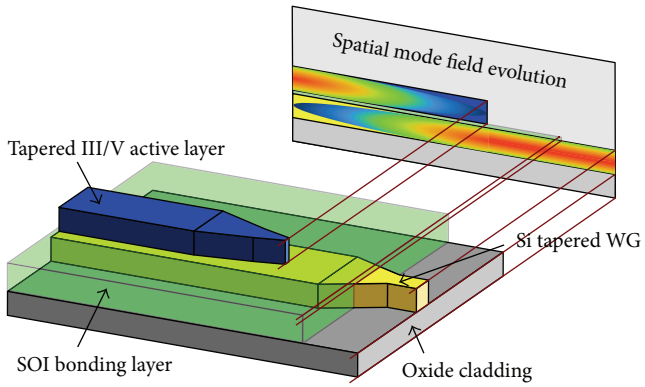

FIGURE 3: Schematic of an adiabatically tapered III/V, silicon laser device. The optical mode is injected from the above WG (blue) into the underlying WG (yellow) using an evanescent coupling. The screen on the figure depicts the exchange of energy between the two superimposed WGs.

To lower the complexity and the difficulty of fabrication of hybrid double taper structure, a DBR-based cavity can also be used in this case to both reflect the cavity mode and couple it to a silicon output waveguide, as demonstrated in [31, 32].

2.2. III/V Colloidal Quantum Dots. As we already discussed in Section 3, semiconducting QDs synthesized by colloidal chemistry are an interesting class of materials to realize a hybrid silicon photonic platform. In fact the chemical synthesis exploits their unique size dependent optical properties and permits to vary their properties at will and thus to cover a broad range of applications.

For the near-infrared spectral range, lead-based colloidal QDs are of considerable interest due to their unique optical and electronic properties [33, 34]. Their absorption and emission wavelengths depend on the dot size, which can be easily controlled during chemical synthesis. Therefore, they are very attractive as building blocks for nanophotonic applications at telecommunication wavelengths. Especially lead sulfide (PbS) quantum dots have found a wide range of potential applications such as active materials in mode locked laser [35], surface emitting lasers [36], polymer strip-loaded plasmonic waveguides [37], and solar cells [38].

A convenient way to manufacture stable and reproducible quantum dot based devices is to introduce the quantum dots into polymers like PMMA, SU-8, or PFCB [39]. In fact, by choosing the proper ligand, the quantum dots can be dispersed into various polymers that act as a matrix in which the quantum dots are homogeneously distributed [40, 41]. The choice of a polymer that can be structured by photo-, electron-beam, or soft lithography opens the possibility to fabricate photonic devices from this hybrid material. Furthermore, inorganic surface capping of colloidal nanocrystals was achieved recently, allowing the encapsulation of the quantum dots into an amorphous As_2S_3 matrix, which resulted in an all-inorganic thin film with stable infrared luminescence in the telecom region [42].

Recently, Humer et al. demonstrated the coupling of the emission of PbS quantum dots into the resonating modes of SOI ring resonators on an all-integrated optoelectronic chip [40]. Such results are presented in Figure 4. An optimal spontaneous emission rate enhancement ratio of 13 was found in TM polarization and linear dependence on the excitation intensity was also found up to 1.64 kW/cm^2 without degradation of the intrinsic resonator Q factor. Solid and vertically slotted cavities were also recently compared in terms of Q factors and ideal Purcell factors [43]. In both these two last articles, the authors also observed that the polymer-quantum dot blends showed unaltered performance weeks after preparation, indicating the high stability of this composite material. It is important to note that, as the emission wavelength of chemically synthesized quantum dots can be precisely controlled, the working bandwidth of quantum dot based optoelectronic chips can be easily tuned to other wavelength regions within the transparency region of the Si waveguides. In another recent article, Omari et al. analyze the absorption coefficient of SOI planarized waveguides coated with mono- and multilayers of PbS/CdS quantum dots by combining

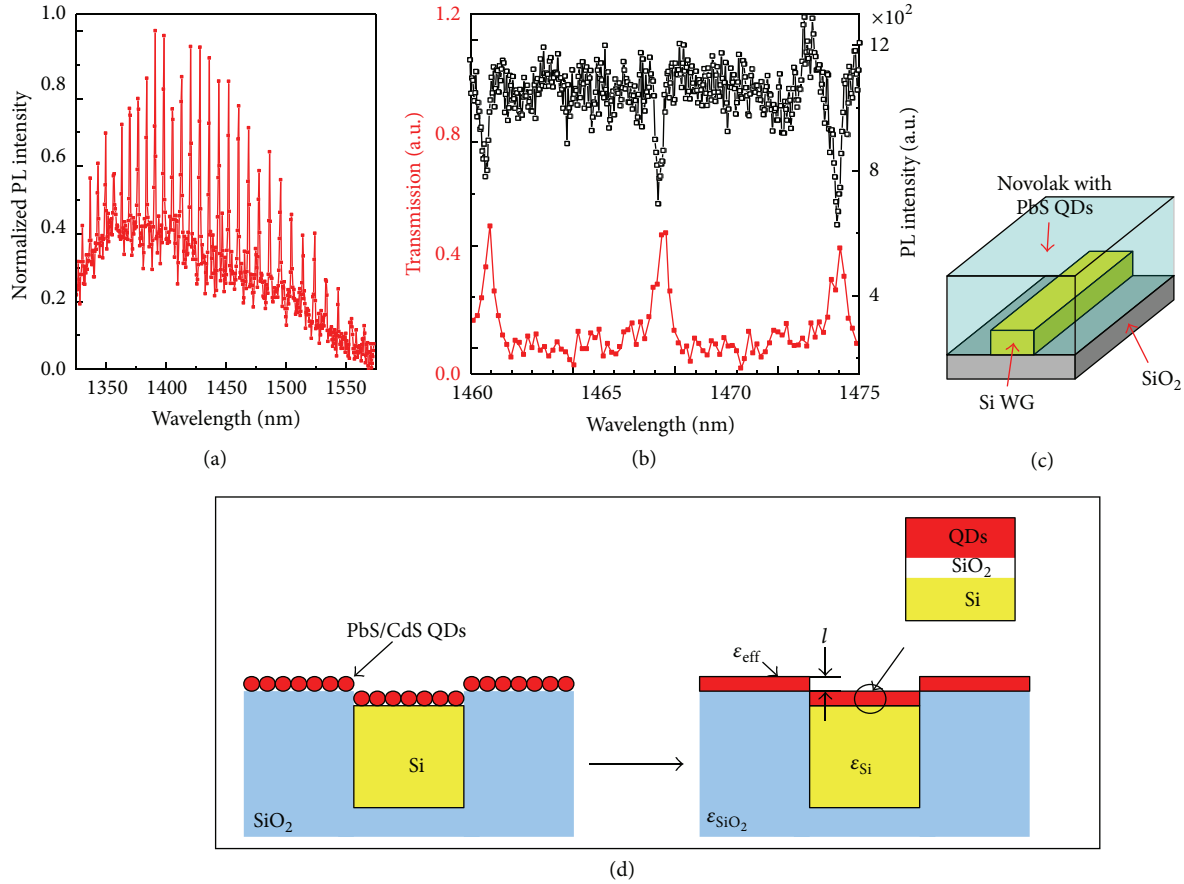

FIGURE 4: (a) Room temperature PL spectrum of Novolak containing 4 vol% of PbS drop cast onto the RR collected at one output facet of the WG. Ring modes correspond to the narrow peaks of the PL spectra which are superimposed to a broad background coming from the WG (Data courtesy of Dr. R. Guider).

optical lithography and Langmuir-Blodgett deposition [44]. The results of this investigation are presented in Figures 4(c) and 4(d). By combining experiments and simulations, they were able to study the variation of the host dielectric constant in function of the NC layer thickness, which is crucial for the optimization and development of quantum dot based devices.

2.3. Nonlinear Optical Properties. Concerning photonic applications like optical switching, holography gratings, or spectral filtering, materials with a large nonlinear refractive index n_2 at telecom wavelengths are needed. Table 1 reports the values of n_2, β, and their FOM for typical bulk semiconductors, chalcogenide glass, and nonlinear polymers at telecom wavelength ($\lambda = 1.55\,\mu$m) taken from recent literature.

It is shown that materials such as GaAs, Si, or silica have very low FOM at telecom wavelengths, which make them hardly suitable for photonic applications listed above, and on the other hand, materials with high FOM like AlGaAs or chalcogenide glass are barely applicable for extensive production, due to their high cost of fabrication. In the same article, the authors experimentally demonstrated that PbS quantum dots have FOM larger than the one at $\lambda = 1.55\,\mu$m, which is comparable to the values found for chalcogenide glass and much higher than the one of GaAs, Si, or silica. This fact clearly renders III/V QDs to be of interest as active materials to fabricate nonlinear optical devices.

By modification of the surface of the quantum dots, it is also possible to tune their optical properties. For example, in the case of PbS, Abel et al. demonstrated that the photoluminescence quantum yield increases by a factor of two by adding trioctylphosphine as a capping molecule [45]. Another possibility is the fabrication of a protective crystalline shell, in order to form PbS/CdS core shell nanocrystals. These structures are really promising, as evidenced by their fabrication by several groups worldwide [46, 47].

The main disadvantage of several of these quantum dots is their toxicity. For example, in the case of PbS, it is well known that, as PbS oxidizes to Pb^{2+} ions in presence of water, it can be the origin of many serious diseases, including cancer [48]. By encapsulation of the QDs by a SiO_2 shell, it is possible to reduce the cytotoxicity of the quantum dots by more than one order of magnitude [49, 50]. Nevertheless, the photoluminescence intensity of the NCs notably degrades by the growth of such a shell, because of the oxidation of the QD surface [49, 51]. The growth of a crystalline shell is therefore essential in order to preserve the optical properties of the quantum dots during the SiO_2 shell formation.

Table 1: The nonlinear refractive index n_2, the nonlinear absorption coefficient β, and figure of merit (FOM) for typical materials measured around $\lambda = 1.55\,\mu$m.

Material	n_2 [10^{-13} cm^2/W]	β [cm/GW]	FOM [$n_2/\lambda\beta$]
Fused silica [55]	0.0027	⋯	⋯
Semiconductors			
Si [56]	0.45	0.79	0.37
GaAs [56]	1.59	10.2	0.1
AlGaAs [57]	1.75	0.35	3.2
Chalcogenide glass [58]			
$Ge_{25}As_{10}Se_{65}$	0.6	0.4	1.0
$Ge_{33}As_{12}Se_{55}$	1.5	0.4	2.4
$Ge_{35}As_{15}Se_{50}$	24.6	0.5	3.2
$As_4S_3Se_3$	1.2	0.15	5.0
$As_{40}S_{60}$	0.6	<0.03	>12.0
Polymers			
DDMEBT [59]	1.7	⋯	2.19

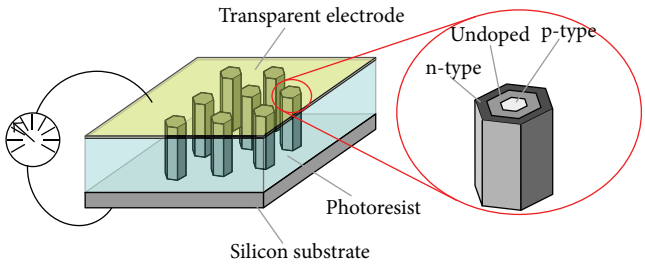

Figure 5: Schematic of the vertical single-nanowire radial pin device connected to a doped silicon wafer by epitaxial growth. The right part of the figure sketches the doping structure of the nanowire. The p-type doped core is in contact with the doped silicon substrate and the n-type doped shell is in contact with the top transparent electrode (ITO), adapted from [60].

2.4. III/V Silicon-Based Hybrid Solar Cells. The last devices that we will discuss in this section are the hybrid nanowire based solar cells, which are a promising approach for third generation photovoltaics. Recently, new concepts of solar cells based on arrays of microwires demonstrate large improvement in the photovoltaic cell performance. In particular higher absorption compared to that obtained in similarly textured films was demonstrated [52, 53]. The main limit of these proposals relies on the limited total absorption rate, even in the case of arrays of highly absorbing nanowires [54].

Recently, Krogstrup et al. presented a concept of a single standing GaAs nanowire solar cell grown on a silicon substrate, where the top and the bottom contacts are made of transparent electrode and the silicon substrate, respectively [60]. The design of such structure is presented in Figure 5. Under illumination, their device shows a photogenerated current density of 180 mA/cm^2 and solar conversion efficiency of 40%. Table 2 compares the current best values for solar cell devices, like single-junction crystalline silicon (c-Si) and GaAs, and nanowire based device. The nanowire based device sustains a very large current and its performance is mainly limited by a small V_{OC} and filling factor (FF). But the authors observed a light concentration effect and a significant increase in absorption rate close to the band gap which can definitely decrease the entropy in the energy conversion, from radiant light into electrical work. They also noticed an increase in the absorption cross-section, which could allow larger separation between each nanowire on the final device. According to these observations, this single standing GaAs nanowire solar cell grown on a silicon substrate could have great perspective in the field of third generation solar cells.

Table 2: J_{SC}, FF, V_{OC}, area, and efficiency η of the best photovoltaic technologies compared with the standing nanowire configuration presented by Krogstrup et al., adapted from [60].

Technology	J_{SC} [mA/cm^2]	FF [%]	V_{OC} [V]	η [%]
c-Si	42.7	82.8	0.706	25
GaAs	29.68	86.5	1.122	28.8
Nanowire device	180	52	0.43	40

3. Fabrication and Integration of Hybrid Materials into Photonic Devices

This section gives an overview of the fabrication technologies that enable the integration of III/V and II/VI materials to create passive and active hybrid devices.

3.1. Standard Silicon Photonics Fabrication Processes. The study of photonic devices has shown in the last fifty years incredible progress. Today, most optical active components are made from IIIV-based compounds, like indium phosphide (InP) or gallium arsenide (GaAs), and are often custom-made and assembled from discrete components. The net result is that these optical devices are relatively expensive. Silicon photonics is a viable way to tackle the problem by developing a small number of integration technologies with a high level of functionality that can address a broad range of applications. Over the last years, the silicon photonics community has made tremendous progress in implementing a large variety of optical and electrooptical devices in silicon, leading to important discovery in fields like biosensing, optomechanics, and nonlinear optics [61]. All these technological advances have in common the fact that they are based on the silicon on insulator technology, which allows the high optical mode confinement of the silicon waveguides.

As mentioned above, the great advantage of the silicon-based technology relies on its compatibility with the actual CMOS fabrication equipment and several companies (Intel, Leti, AMO, and IMEC), which are now leaders in the field of the fabrication of silicon-based photonic components, use such technology to develop their products [62].

Most of these companies employ wafer-level process technology, which allows them to manufacture high volumes of highly precise and state-of-the-art nanophotonic and optoelectronic systems on a single wafer. The benefits of

this process technology include economies of scale, fast ramp to high production volumes, high levels of integration and miniaturization, and precise location of microstructures. However, some companies, as well as many research centers, use small-scale manufacturing, which in other words means that the production processes are developed not all over the entire wafer, but only a small portion of it, also called sample. This technique offers many benefits, including economic, especially during the process of development of a device. The manufacturing process of a silicon-based product (or a sample) is usually divided into three parts as follows.

(1) The first part involves the deposition or creation of one or more layer of material on the silicon substrate. This can be performed using different methods depending on the desired material. Among the different techniques available we mention the wafer bonding techniques (e.g., for the fabrication of silicon on insulator (SOI) substrates), the chemical vapor deposition (e.g., for the deposition of amorphous silicon), the molecular beam epitaxy (which is used for growing an ultrathin layer of a semiconductor or organic semiconductor on Si substrate in order to create Si-based heterostructures), and the sputtering techniques.

(2) The second step of the manufacturing process consists in the definition of a desired pattern via a resist deposited on top of our sample. Such a process is usually done using a lithographic step. The minimum feature size, required by the fabrication of the device, determines the type of the lithographic technology: photolithography (features size below 50 nm using 193 nm ArF line and immersion techniques) [63], nanoimprint lithography (sub-10 nm feature size) [64], and electron-beam lithography (features size of 2 nm [65]) are the most common ones. After this process, the sample can also be redirected versus another deposition process, like for the lift off technique.

(3) The last step of the manufacturing process is the transfer of the pattern from the photoresist to the sample through an etching procedure. Reactive ion etching (RIE), inductively coupled plasma RIE, and chemical etching are the most common techniques use for this purpose.

3.2. Integration of Hybrid Materials into CMOS Technology. Using such technology, we are now able to create high quality Si-based components like low loss waveguides, grating couplers, and photonic crystal devices [66].

Unfortunately, the Si photonic approach is challenged by several fundamental and technical problems to create active devices such as lasers, amplifiers, and modulators [67]. The main one is the fact that Si is an indirect band gap semiconductor, posing major difficulties in the concepts of Si-based electrooptical modulators and light emitters. Another important aspect is the operating wavelength range, which in the case of Si is limited in the near- to medium-infrared range (e.g., between 1.2 and ~6 μm).

A solution to overcome these problems is to create hybrid systems using materials with properties offsetting the silicon limits. To this end III/V materials add to the Si photonic platform fundamental properties like efficient light emission and high speed modulation capabilities [68]. Materials like optical polymers can also be integrated into Si chip in order to create high-speed signal processing due to their high third-order nonlinearity or even low-temperature heterojunction solar cell [66, 69].

3.3. Integration of III/V Semiconductors via Wafer-Scale Strategies. A first process to create hybrid photonic products is to integrate directly III/V based materials onto silicon-based wafer. This can be done using low-temperature wafer bonding techniques, which are not subject to the lattice matching limitations associated with epitaxial growth and the precise alignment and sequential attachment of individual devices in the flip-chip technique [25].

The bonding of III/V materials onto silicon on insulator waveguides (Figure 6(a)) has given remarkable results in this last decade, enabling the fabrication of hybrid AlGaInAs and InP-based lasers, but has also to face the inefficient use of the III/V layers and the wafer size mismatch [70]. The die-to-wafer bonding technique is also able to transfer III/V epitaxial layer structure to SOI waveguide circuit by a die-to-wafer bonding process using either molecular bonding or an adhesive bonding approach, like the thermosetting polymer divinylsiloxane benzocyclobutene DVS-BCB (Figure 6(b)) [71]. However both high topographic features and the lack of the positional tolerance and capability for parallel processing required for high-volume production continue to be an issue for the adoption of this technology.

Another bonding technique used to transfer preprocessed photonic III/V devices on SOI waveguides is the metallic bonding. Using such concept, the realization of hybrid lasers like InGaAsP-Si laser was demonstrated with impressive results, but their fabrication requires also precise alignment (submicron precision bonding procedure) [72].

Recently, Justice et al. introduced a wafer-scale strategy for the integration of high-performance GaAs lasers on non-native substrates [73]. The process is sketched in Figure 6(c). After patterning and etching of a dense array of defined areas (coupons) on the epitaxial wafer, a wafer-scale microstructured elastomeric stamp is used to selectively release and transfer the 5.7 μm thick coupons of epitaxial material to a silicon host wafer by transfer printing. This strategy results in a wafer-scale planar process with posttransfer lithographic alignment and a low thermal budget while making efficient use of the IIIV epitaxial material.

3.4. Colloidal Quantum Dots Integration. Another promising class of materials for integration into silicon photonic chips is the class of semiconductor quantum dots (QDs) that are synthesized by colloidal chemistry. QDs display discrete atomic-like electronic level structure with intense optical dipole transitions. As their absorption and emission wavelength depend on the dot size, which can easily be controlled during synthesis, they are extremely attractive as building

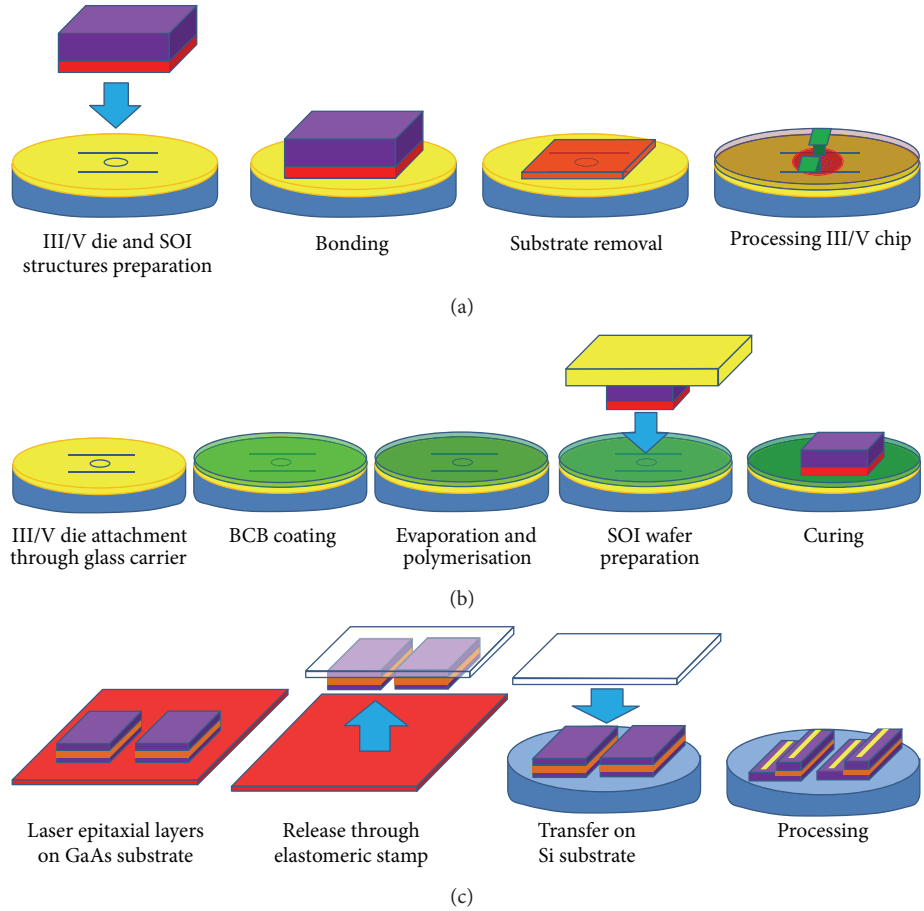

Figure 6: Process flow of the hybrid device fabrication with the (a) III/V (unprocessed) die-to-wafer technique, (b) DVS-BCB bonding technique, and (c) transfer printing technique.

blocks for nanophotonic applications. Nowadays, they have found a wide range of potential applications in biosensors, chemical sensors, photovoltaic cells, light amplifiers, and light emitting diodes [33, 34]. Recently, it was also demonstrated that such materials have also a large nonlinear refractive index n_2 at telecom wavelengths, which raises a large interest in their possible application as nonlinear optical materials for photonics (e.g., like for optical switching, holography gratings, and spectral filtering).

With regard to their integration in a photonic integrated circuit, the fabrication of a QDs-based waveguide will provide a flexible platform to exploit their optical properties. Nowadays, a convenient and easy way to produce stable QDs-based waveguide is to mix them into suitable polymers like PMMA or PFCB [36, 37]. In fact, by choosing a proper ligand, the QDs can be simply mixed into various solvents and organic polymers.

In this way a homogeneous dispersion of polymers and QDs can be formed and spin coated in thin films on substrate surfaces. After solvent evaporation, the polymer acts as a matrix into which the QDs are homogeneously distributed [38, 39]. For optoelectronic applications in the telecommunication region, we are particularly interested in polymers that are transparent at these wavelengths, that are easily structured with and compatible with Si-based technology, and that can be cured at low temperature, so that they do not affect the optical properties of the QDs.

However, the dispersion of the nanocrystals in solid polymer matrix is frequently hampered by phase separation and nanocrystals aggregation, which results in heavy degradation of the luminescence properties or even of the total quenching of the emission and thus in a serious degradation of their active properties.

In the last years, Humer et al. investigated these effects by introducing PbS QDs into different polymer matrices and demonstrated recently the spectral and intensity stability over weeks for PbS QDs mixed into Novolak polymer [40], which evidences the feasibility of such a method in the fabrication of a stable hybrid photonic integrated circuit.

A hybrid strategy similar to the one discussed above but based on PFCB and PMMA polymers was used to create low loss multimode waveguides at 1.5 μm [36]. Another application of this procedure at telecom wavelengths was to create a polymer strip-loaded plasmonic waveguide doped with nanocrystals, to investigate the gain-assisted propagation by stimulated emission [37].

In order to create the finale device, the QDs mixed in polymer need to be deposited on the silicon chip, which

can be achieved by several methods, like evaporation-induced self-assembly, drop casting, template patterning, and Langmuir-Blodgett (LB) or Langmuir-Schaeffer deposition [74]. These last two techniques can be used to selectively deposit quantum dot monolayers on patterned surfaces and to achieve micrometer resolution after the lift-off of the lithographic mask.

Using lithographic methods, some polymers also allow the integration of QDs on Silicon Wafer by acting as a host material where the QDs are mixed. A compound material suitable for device applications should consequently ensure high stability over a long period of time while still preserving the sensitivity to lithographic patterning. Recently, novel epoxy-based photoresists like SU8 or mrL 6005 XP have been shown to also keep their lithographic processability after the incorporation of the nanocrystals (NCs) emitting in the visible wavelength regime [75, 76]. Humer et al. recently demonstrated that the spatial definition of spincast PbS quantum dots embedded in polymer film by EBL is possible without degrading the emission properties of the NCs [43]. The compound additionally showed unaltered optical properties weeks after sample preparation, pointing out the high stability of this material and its suitability for device applications at telecom wavelength.

4. Integration of Graphene in Silicon Photonics

Since a decade ago and its isolation by mechanical exfoliation [77], graphene has been the subject of numerous studies from the scientific community, leading to the discovery of its extraordinary properties. We will now describe here some of them and show how they can be implemented in the field of hybrid integrated photonics.

Concerning its optical properties, Nair et al. stated that the graphene opacity was of 2.3% for a single atom thick layer and in a very large range of wavelengths including visible and near-infrared region [78]. Such property lies in the two-dimensional nature and gapless electronic spectrum of graphene. Another interesting property of this material is its extremely high charge-carrier mobility which allows ultrafast extraction of light-generated carriers [77, 79] and also perfect charge-carrier confinement [80, 81]. Taking into account all these characteristics, graphene is an ideal candidate for the realization of ultrawide-bandwidth optical modulators and photodetectors.

Regarding its nonlinear properties, Hendry et al. demonstrated that, due to the interband electron transitions, graphene exhibits very strong $\chi(3)$ nonlinearities in the near-infrared spectral region, which are 8 orders of magnitude larger than the one observed in insulating materials [82]. Combined with silicon optical microcavity, this property suggests the creation of new high-performance devices for chip-scale optical physics and ultrafast optics in optical information processing.

By exploiting graphene both as a semitransparent electrode and as an antireflection coating, it is possible to create a hybrid graphene/silicon solar cell and thus create a new class of photovoltaic devices [83]. Finally, in case of porous silicon, it is also possible to use and employ graphene as coating for the fabrication of electrochemical supercapacitor with high electrochemical stability [84].

4.1. Graphene/Silicon Photodetectors. Recently, several articles were published on the realization of hybrid graphene/silicon on chip photodetectors, with high performance and working on a spectral range that covers from the near to the medium infrared [85]. Using the advantages of silicon waveguides, which have low loss and large bandwidth, it is possible to guide the optical mode into these waveguides and at the same time create electron-hole pairs in the graphene sheet, which is located in close proximity. Using such concept different implementation processes were recently proposed and each of them achieved very promising results.

In the first one, by Gan et al. [86], the Si WG optical mode couples to the graphene layer, deposited on top of it, and thus generates photocarriers. To collect the photocurrent created, two metal electrodes were positioned in opposite sides. A scheme of such design is presented in Figure 7(a). One of the electrodes was positioned closer to the waveguide in order to create a potential difference in the graphene to couple with the evanescent field of the waveguide. Such asymmetry helps obtain high internal quantum efficiency for collecting the photocarriers. In terms of performance, they measured responsivity of 0.11 AW^{-1} from 1,450 nm to 1,590 nm and internal quantum efficiency at zero bias voltage of 3.8%.

In the case of the second article, by Pospischil et al. [87], the source electrode was placed directly on top of the waveguide and the two ground electrodes are placed several microns far from it, as shown in Figure 7(b). In this case, a ground-source-ground configuration is used in order to double the value of the total photocurrent measured in comparison to a ground-source scheme. In terms of performance, the measured responsivity is of 0.05 AW^{-1} from 1,310 nm to 1,630 nm and the estimated internal quantum efficiency is of the order of 10%.

Finally, in the last article by Wang et al. [88], the authors used a suspended membrane waveguide to avoid absorption of midinfrared light by the buried oxide (BOX) and to take full advantage of the transparent wavelength region of silicon. A sketch of such design is presented in Figure 7(c). To collect the photocurrent created, two gold electrodes were positioned above the graphene and silicon waveguide with a gap of 1.5 μm. Concerning the performance of such design, the authors found responsivity of 10^{-4} AW^{-1} in the near-infrared region and 0.13 AW^{-1} for the midinfrared region.

Concerning the response of the device, Wang and Posposchil experimentally demonstrated the working principle of their device at 20 GHz but estimated the possibility of working at much higher frequency, as the extremely high carrier mobility of graphene is estimated to result in an intrinsic photoresponse faster than 640 GHz [89].

It is important to note that all these three articles represent promising results in the field of integrated photonic devices, by combining the extraordinary properties of graphene material with the CMOS technology. They associate high-speed operations with large band detection range and ultrasmall

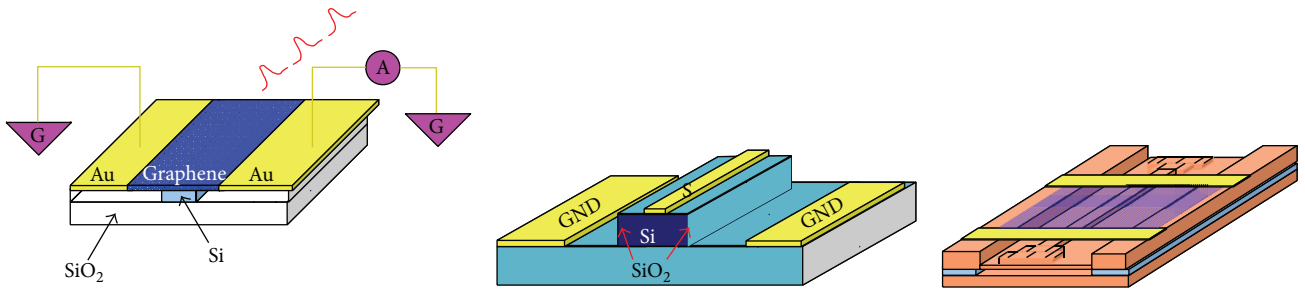

FIGURE 7: (a) Schematic of a waveguide-integrated graphene photodetector. (b) Cross-section sketch of a waveguide-integrated graphene photodetector device. The active region of the graphene sheet is shown in violet. (c) Schematic of graphene/silicon-heterostructure waveguide photodetector.

device, which can suggest the birth of a complete new category of high-performance photodetectors.

4.2. Hybrid Graphene/Silicon Optical Cavity. As we have just described the integration of graphene in CMOS photonic devices for the realization of promising photodetectors, another intrinsic property of this material, for example, its nonlinearity, could allow for the fabrication of really high quality optoelectronic devices.

In order to achieve all-optical signal processing like spectral filtering or optical switching, materials with large nonlinear susceptibility or, equivalently, a large nonlinear refractive index n_2 are required. In this case, the index of refraction n of the material is related to the intensity I of the radiation field by $n(I) = n_0 + n_2 I$, where n_0 is the linear refractive index. The nonlinear refractive index alone is not a suitable parameter to determine the usefulness of a nonlinear optical material. In fact both the real and the imaginary parts of the index depends on the incident field; thus the comparison has to be done considering both these elements. A typical figure of merit (FOM) is defined as the ratio between the nonlinear refractive index and the nonlinear optical absorption coefficient: n_2/β. At telecom wavelengths, typical bulk semiconductors have only a small FOM [56] (Silicon: FOM = 0.37; GaAs: FOM = 0.1). These small values are not sufficient to induce a strong optical Kerr effect. On the other side, materials with high FOM like AlGaAs or chalcogenide glass (AlGaAs: FOM = 3.2; $Ge_{33}As_{12}Se_{55}$: FOM = 2.4) are really inconvenient due to their high cost of processing and fabrication.

Because its symmetry graphene has vanishing 2nd order susceptibility [90], Hendry et al. demonstrated that it exhibits very strong $\chi(3)$ nonlinearities in the near-infrared spectral region [82] due to the interband electron transitions. Using such properties, Gu et al. recently fabricate a hybrid graphene/silicon cavity by transfer of a graphene monolayer sheet to air-bridged silicon photonic crystal nanomembranes [91]. A sketch of such structure is represented in Figure 8.

With this device, they demonstrated the really high 3rd order nonlinear response of graphene and exploited it to achieve ultralow-power optical bistable switching, self-induced regenerative oscillations, and coherent four-wave mixing at femtojoule cavity energy on a semiconductor chip platform. From their experiments, they estimated the Kerr coefficient of their hybrid graphene/silicon cavity to be of about $4.8 \cdot 10^{-17}\ m^2W^{-1}$, which is one order of magnitude larger than that in monolithic silicon and GaInP-related materials and two orders of magnitude larger than that in silicon nitride [92, 93]. Using also a hybrid graphene/silicon cavity, Majumdar et al. demonstrated changes in the photonic crystal cavity by electrostatic gating of a single layer of graphene on top of it as they observed a shift and a linewidth increase of the cavity resonance [94]. They also measured the speed of their device to be of 20 GHz but estimated to work also at over 100 GHz. With these results, the authors claimed that such hybrid graphene/silicon cavity design could be used as a modulator at very low power (in the order of fJ) and so open new possibilities in the field of high-speed silicon-based modulators.

4.3. Graphene/Silicon Solar Cells. In the field of photovoltaics, promising devices were recently proposed using the properties of innovating materials like carbon nanotubes, with really encouraging results [95–97]. These devices benefit from the superior optoelectronic properties of carbon nanotubes coupled with the well-developed technologies in the field of silicon photovoltaics. Using such approach, devices with power-conversion efficiency up to 11% were recently demonstrated [97].

Concerning graphene material, Li et al. demonstrated in [98] the realization of a hybrid graphene on silicon Schottky junction solar cell, where the authors deposited graphene sheets on top of a Si/SiO_2 wafer (Figure 9). A scheme of such device is presented in Figure 3. The characterization of the solar cell was done under air mass 1.5 illumination, and overall solar energy conversion efficiency of 1.7% was found. This value is still far from the one of silicon or even carbon devices reported in [99] mainly because the graphene sheet acts as an antireflection coating, but the authors claimed that there is still place for large improvement of their device performance. The open-circuit voltage V_{OC} can be increased by surface passivation of the silicon and by a proper optimization of the tradeoff between conductivity and transparency of the graphene layer. Such results, even if still below the standard ones of photovoltaic materials are really encouraging for the conception of a new type of hybrid device

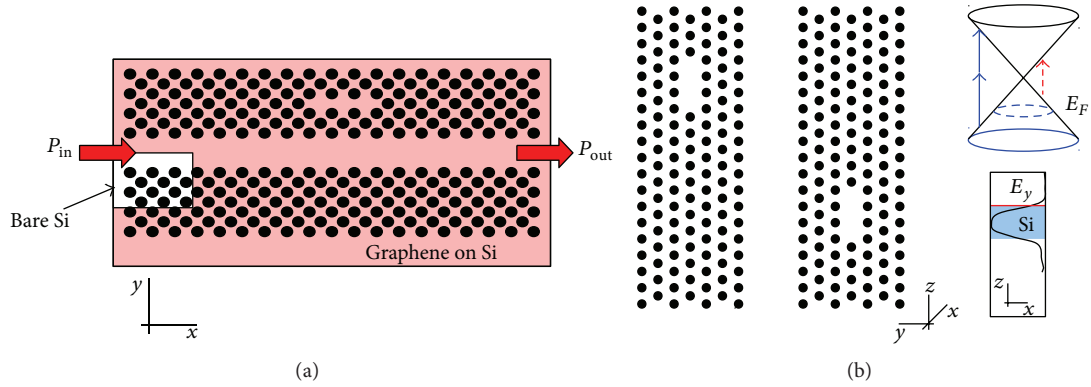

FIGURE 8: (a) Sketch of the tuned photonic crystal cavity, with lattice constant $a = 420$ nm. (b) Sketch of the suspended graphene/ silicon membrane. Top right inset: Dirac cone illustrating the highly doped Fermi level (dashed blue circle), allowing the two-photon transition (blue arrows) but forbidding the one-photon transition (red dashed arrow). Bottom right inset: computed Ey-field along the z-direction, with graphene at the evanescent top interface.

that exploits the advantages of graphene intrinsic electric field properties to fabricate simple and cheap photovoltaics [83].

4.4. Graphene Porous Silicon Electrocapacitor. Finally we describe a new type of graphene/silicon-based hybrid material fabricated using porous silicon (pSi) substrate. In fact, pSi is a material with really interesting properties like a large surface area (up to 800 m^2/g) and tunable optical properties, which have found application in the fields of sensing and detection of biomolecules [100]. Concerning the fabrication of such material, controlled electrochemical techniques allow nowadays a fine supervision of the surface area, the porosity, and the pore morphology of the semiconductor [101]. In an article published recently, Oakes et al. report the fabrication of stable electrodes for electrochemical devices using porous silicon coated with an ultrathin graphene layer [84]. They characterized their capacitors by performing charge-discharge measurements and electrochemical testing and observed energy densities of 2.5–3.5 Wh/Kg, which are similar to the ones of carbon-based supercapacitor currently available in the market. Such a device looks quite promising for the fabrication of high quality energy storage device and thus opens up new opportunities in the field of porous based materials and integrated device for applications like sensing and photovoltaics, where the integration of efficient energy storage material into existent silicon-based technology platforms is needed.

5. Organics

This section describes the recent achievements obtained in optoelectronics and photonic exploiting organic based materials. Organics have a huge potential in the development of next generation of both photonic and optoelectronic devices. Their molecular structure and the possibilities given by the chemical synthesis to modify their composition at molecular level allow for a fine tuning of their optoelectronic properties over a broad range. Two classes of materials are discussed in this review: polymers and molecular organic semiconductors.

Polymeric materials are often exploited to add complex functionalities to silicon photonic devices. Their large thermooptic coefficient is exploited to realize athermal ring resonators that do not require an active trimming to compensate for the drift in wavelength resonance due to temperature variations. This is an important step towards the realization of optical networks working at Tb/s because it greatly reduces the amount of power consumed.

On the other hand optically active organic semiconductor is an extremely active research field and the improvements in its optoelectronic properties (and lifetime) have finally brought the commercialization of products based on them (like OLED and active matrix OLED display for mobile electronics). Thus active optoelectronics is already a well-established technology and its integration with silicon (and more generally) inorganics based technologies will further increase its possibilities.

5.1. Polymers in Silicon Photonics. Polymeric materials are seldom considered as candidate material for integrated photonics. This is mainly due to the fact that their small refractive index limits the confinement of the optical modes and thus the level of integration of polymer based photonics is somewhat limited. Moreover optical losses in the telecommunication spectral windows are much larger than those of silica fibers (they are in the order of 0.02 to 0.1 dB/cm at 840 and 1550 nm, resp.) [102, 103].

Despite these fundamental limits polymers have good potentiality in all the cases where tight confinement of the guided mode and long distance transmission are not key issues [104, 105]. In fact polymers can be synthesized with well controlled and broadly tunable chemophysical properties [106]. They are often easy to mold and polymeric photonic circuits can be fabricated with a number of different technologies (optical lithography [107, 108], imprinting/embossing [109, 110], and photoreaction and nonlinear optical induced polymerization [111] to cite the most investigated ones). In the last years polymeric materials were integrated into nanophotonic devices to exploit their peculiar properties, in particular their highly nonlinear optical coefficient.

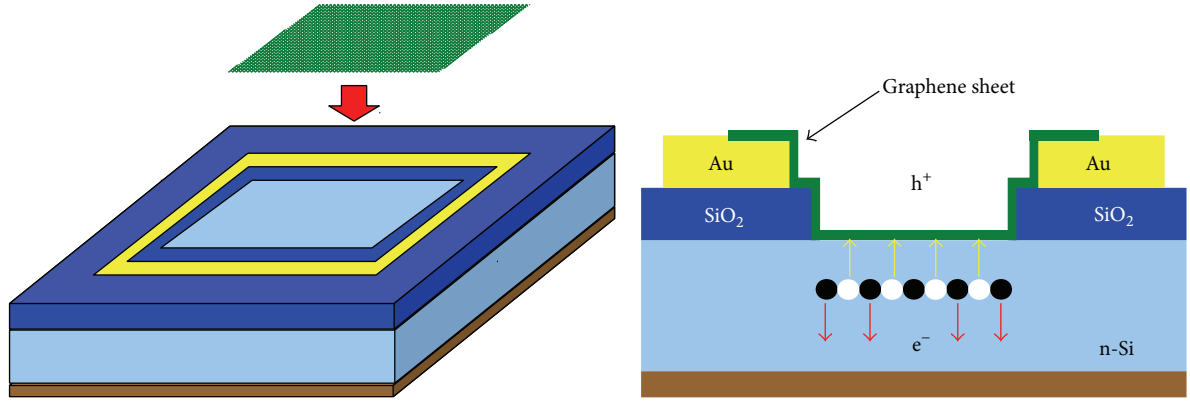

FIGURE 9: (a) Schematic illustration of the device configuration. The graphene layer is deposited on top of the silicon substrate. Gold electrodes were deposited previously. (b) Cross-sectional view, from [98].

One of the most studied cases considers their use to develop high-speed electrooptic modulator [112]. It is well known that the cubic symmetry of the silicon lattice forbids the appearance of 2nd order nonlinear properties, and even if the 3rd order coefficient is quite large, its usefulness is still limited by two-photon absorption mechanism [113, 114]. Thus despite being the ubiquitous material for the integrated photonics of the coming years, it certainly needs to be coupled with other materials to include nonlinear functionalities and exploit the full potential of integrated photonics.

The small refractive index dispersion of polymers permits to achieve large modulation bandwidth. Modulation frequencies up to 100 Gbs were demonstrated in [115–119].

Several different polymers were so far investigated [120], and the most recent implementation of electrooptic modulators shares a common geometry based on slot WG filled with a nonlinear polymeric material [121–124]. Slot WG is a particular type of WG able to confine a large part of the guided mode field within the low index region [125]. Initially they raised a large interest mainly for high refractive index materials. In fact the field enhancement within the slot region originates from the discontinuity of the component perpendicular to the slot internal surface (the horizontal component). And its intensity scales up as the square of the refractive index contrast between the two materials that compose the slot WG. Later on it was demonstrated that the simple ratio among the refractive index of the materials that compose the WG does not describe completely the behavior of the slot and that several applications (like optical gain [126] and sensors [127]) require a more careful design of the WG geometry to maximize their performance. In particular when medium to low index materials are considered as slot WG material, the slot can be wider because the decay length of the evanescent field is longer (albeit its absolute intensity is lower) and thus the integral of the field within the slot may be greater than the one obtained in high index materials. Figure 10 reports the calculated confinement factor (defined as the fraction of the field confined within the slot region) for slot WGs made of high and low index materials. The data clearly show that for extremely narrow slots high index materials achieve higher field confinement within the slot volume. This is due to the higher discontinuity of the field component at the interface. On the other hand low index materials (like polymers and glass) perform better at larger slots width because the longer evanescent tail can be used to enhance the value of the integral. These two regimes may be differently exploited depending on if either the field intensity or the power density is the key parameter for the desired application.

Figure 11 reports 3D rendering of a typical slot WG; it is made of two dielectric walls (in green) that surround a low index trench. A snapshot of the horizontal field component of a monochromatic continuous source of light sent along the slot WG is depicted in red and is clearly confined within the dielectric walls. The field is concentrated and piled up within the central trench due to the joint effect of the subwavelength size of the two lateral WG walls and the overlap of the exponential decaying field tails within the slot. Thus the slot WG maximizes the interaction between the guided mode and the optical nonlinearity of the material that fills the slot volume. Modulators fabricated with this hybrid system can sustain several tens of Gb/s operations and are a potential candidate to develop the next generation of Tb/s architecture [128, 129] which will have stringent requirements in terms of energy consumption per bit's switching [130, 131]. Due to their large thermooptic coefficient (with the order of $3 \times 10^{-4}/^{\circ}\mathrm{C}$) polymers are investigated also to realize variable optical attenuator (VOA). Despite the thermal degradation shown by the first prototypes proposed, the most recent implementation demonstrates good device reliability and permits the use of low cost polymeric VOA for real applications [132]. Recently an integrated modulator based on the variation of the birefringence of polymer based Mach-Zehnder interferometer was demonstrated [133]. Despite the slow switching speed (ms), limited by the speed of the thermooptic effect, the device shows an extinction ratio of more than 20 dB and a rather good efficiency, being able to induce 2π of phase shift with 70 mW of electrical power.

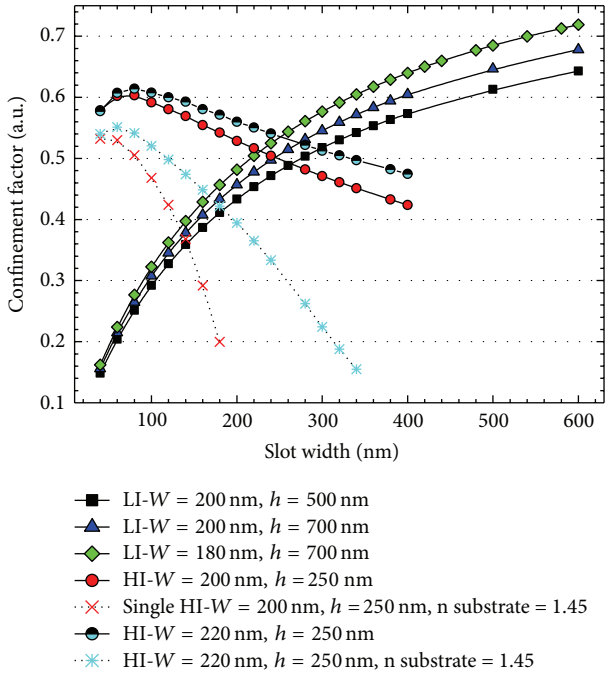

Figure 10: Comparison between the confinement factor of high and low index slot WGs. High index material considers silicon ($n = 3.5$) as the slot walls dielectric, while low index material considers a SU8 polymer ($n = 1.6$). The polymeric slot WGs have a bottom cladding made of a very low index material ($n = 1.2$, a value compatible with xerogels' materials).

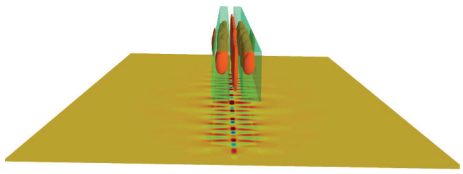

Figure 11: 3D rendering of a slot waveguide and of a monochromatic wave propagating along it. The two green regions indicate the high index volumes that embed the slot. The two evanescent tails of the electromagnetic field pile up within the slot volume and give rise to an enhanced field intensity. For clarity only the electric field component parallel to the horizontal plane is shown and projected below the waveguide structure. The field maxima (sketched in blue and red) are clearly confined within the low index region of the slot.

Polymers were recently investigated also as a cladding material to fabricate passive athermal optical filters [134]. This idea was demonstrated for the first time nearly twenty years ago [135]. In this case the polymer is used as top cladding and its thermooptic coefficient has to counterbalance the one of the underlying (silicon) waveguide. The matching implies that the two TO coefficients must have opposite sign, so that they compensate each other during the device operations. Due to the rather large TO coefficient of the silicon ($1.8 \times 10^{-4}/^{\circ}C$) it is necessary to expand the guided mode so that a relevant percentage of the guided power interacts with the polymer cladding [136, 137]. Recently optimized designs were proposed that avoid the tight fabrication constraints imposed by the use of heavily tapered WG and slot geometries and result in smaller device losses [138–140]. Athermal passive trimming of photonic switches and add-drop filters is of primary importance: the level of integration that will be achieved by IP in the coming years will require an increasing amount of power used to tune each add-drop element resonant with the wavelength it has to route. Both thermal trimming and optical active trimming of these elements need a large amount of power and this fact diminishes the overall power efficiency of the photonic circuit [141]. Thus, in order to minimize power consumption in optical circuits, there is a need for passive and effective trimming technologies.

Compared to the inorganic materials, polymers have small elastic modules. This property is exploited to fabricate mechanically tunable devices [142]. Interesting results in this filed were obtained in [143, 144]. The authors coupled a superluminescent light emitting diode with a tunable Bragg filter fabricated into a polymeric matrix and they showed an extended operational bandwidth of the superluminescent LED under application of either a tensile or a compressive stress to the Bragg structure. The device achieved sub-nanometer tuning step and shows a continuous behavior with negligible fluctuations in the intensity of the lasing mode across the entire spectral bandwidth (of about 100 nm).

5.2. Organic Based Optoelectronics. Since its proposal in early 1980s [145–147] organics optoelectronics is evolving at an extremely rapid pace, driven by the huge possibilities it promises.

This section describes the recent advancements in the field considering the basic building blocks that may be useful in developing hybrid devices in which the active photonics part is performed by organic molecules. Figure 12 shows how the mobility of organic compounds has been improved during the last three decades. The data reported refer to only few commonly investigated materials. It is clear that nowadays the mobility of small conjugated molecules outperforms that of amorphous silicon and these materials are now compatible with a large number of optoelectronic applications that do not require the high mobility typical of integrated circuits and processors. Organic optoelectronics devices can be fabricated using unconventional deposition methods such as inkjet [148], screen [149], and microcontact [150] printing. The low temperature required by these methods makes them fully compatible with plastic substrates and roll-to-roll processes [151]. These are great advantages in terms of both cheapness and energy required by the fabrication method, compared to inorganic based devices. Furthermore the properties of the organic based materials can be defined at molecular level by proper design and addition of functional groups. Thus large tunability in optoelectronic properties is expected.

Organic semiconducting materials can be used to fabricate active optoelectronic devices that aim at substituting their inorganic counterpart (such as in the case of OLED and OLET). Alternatively they can be integrated within an inorganic device to exploit the large flexibility of their optoelectronic properties, to add specific functionalities that are otherwise not attainable in the inorganic host. Below

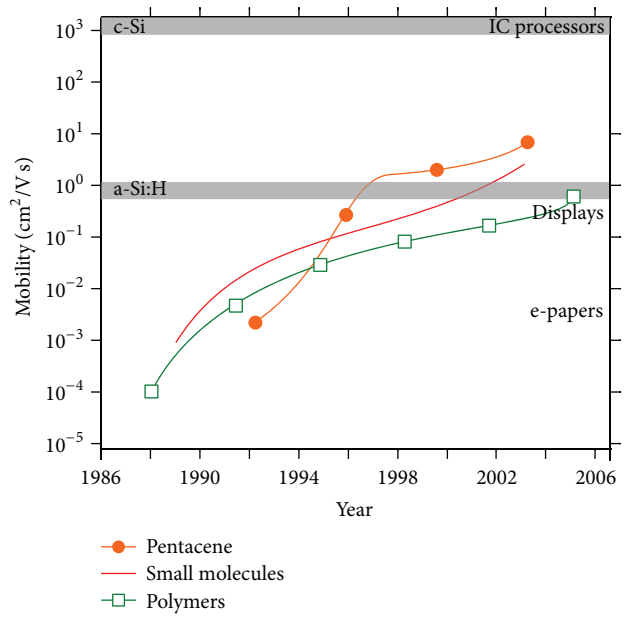

FIGURE 12: Improvement in electron mobility achieved during the last three decades. The mobility was increased by five orders of magnitude and, for selected compounds, is higher than that of amorphous silicon, adapted from [152, 153].

we review some recent achievements in OLED and OLET technologies.

Organic based technologies that are currently the most promising in terms of market exploitation are generally grouped in three categories: organic light emitting diodes (OLEDs) (the first demonstration was published in [154]), organic field effect transistor (OFET), and organic photovoltaics (OPVs). OLEDs bring the development of flat panel display for both mobile and large area screens [155]; OFETs permit fabricating cheap integrated circuits on plastic substrates, in some cases able to rival the inorganic counterpart in term of speed [156]. OPVs have reached efficiencies with the order of 10% that make them attractive for all those applications that do not rely on high efficiency [157, 158]. Besides the fact that their performance is often comparable to that of the inorganic counterpart, organic based devices can be fabricated on flexible substrates and conformal to complex surfaces. This fact, coupled with the high chemical flexibility given by the platform, allows for the fabrication of innovative, biomimetic systems that are easily interfaced with biological organisms, for example, artificial eyes [159].

Active devices based on organics may be classified depending on the size of the molecules that compose them: small molecules, polymers, and hybrids organic/inorganic.

The most promising compounds to develop organic based optoelectronic devices are fabricated using π-conjugated molecular systems. In these molecules the delocalized π electrons, coupled to the packing of the molecules that often pair these orbitals, permit achieving rather large electron mobility. Typically it depends also on the crystalline orientation and may vary by order of magnitude [160–162]. Among the most studied small molecular systems we cite oligothiophenes, rubrene, tris(quinolinolate) Al (Alq3), and poly(p-phenylene vinylene) (PPV).

The deposition of π-conjugated systems is a delicate process. On one hand the weak interactions responsible for their arrangement allow for a number of different techniques to be developed (compared to those required by the deposition of the inorganic materials considered in this review), but on the other hand, organics have poor mechanical properties and are easily damaged by thermal stress. Several deposition methods are available to form thin film of organic semiconducting material and they can be classified into two main categories: deposition from liquid phase and physical vapor deposition. Both methods can be subdivided into several other classes that differ for the instrumental details of the deposition equipment. The liquid phase deposition generally requires simpler fabrication systems which are compatible with large area substrates. On the other hand the high vacuum environment used in many physical based processes permits achieving a better control over the final material properties. Some deposition techniques (like the supersonic molecular beam deposition method) allow also modifying the interaction between the diffusing molecule and the underlying substrate. In fact the molecules may impinge on the substrate with an excess of kinetic energy that they use to diffuse and rearrange into their most favorable configuration. In this way both the crystallinity of the material and the carrier mobility can be engineered [163–165]. Figure 13 reports atomic force microscopy of pentacene thin films deposited with different growing conditions. Both the size and the shape of the crystallites can be modified depending on the deposition conditions and consequently the morphology influences the final performance of the device.

OLEDs are generally fabricated using a multilayered thin film structure: carriers are injected from metallic contacts into the active material where charges recombine and emit photons. From such a simple description several problems can be inferred. High efficiency can be achieved only if carriers possess specific properties once they are injected within the organic material: they must have large mobility; they have to show large recombination rates. Furthermore efficient injection is achieved only upon a proper alignment of the energy levels among the contacts and the organic layers. Given the extremely wide properties shown by organic molecules, each of these key factors needs to be optimized looking at the specific system considered and there are only few, general, rules of thumb to predict/design systems with predefined characteristics. In organics devices, holes mobility is often several orders of magnitude greater than the electronics one [166]; thus a balanced injection of carriers, which is important to achieve high external efficiencies, requires a proper design of the device and in this context the multilayered structure allows for a certain degree of flexibility [167, 168].

Figure 14(a) reports a pictorial view of an OLED cross-section with the main layers (sometimes hole and electron blocking layer are also added to improve the efficiency of the recombination within the emitting layer). Figure 14(b) depicts the typical arrangement of the electron energy levels in each layer. It is clear that proper matching of the energy

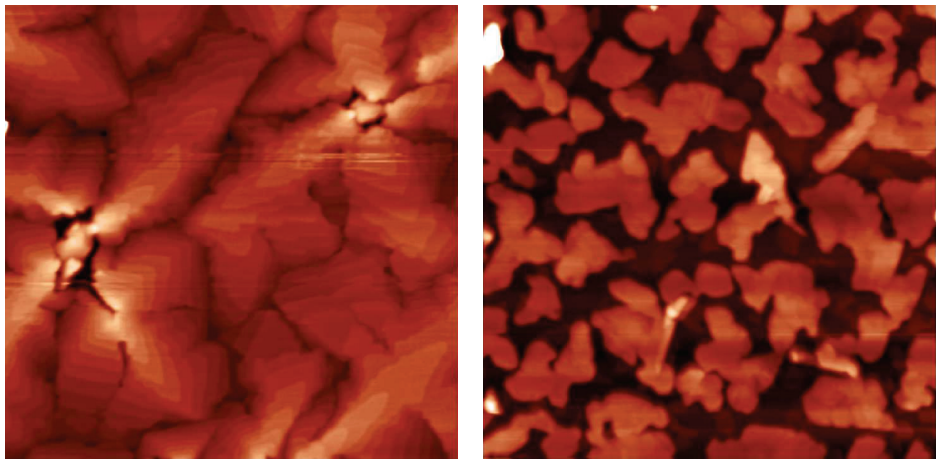

(a) (b)

Figure 13: AFM of two pentacene layers deposited by supersonic molecular beam at different growing conditions. In both cases the thin film growth creates islands but both their shape and size can be modified by properly tuning the deposition conditions. Both images are $5 \times 5\ \mu m^2$.

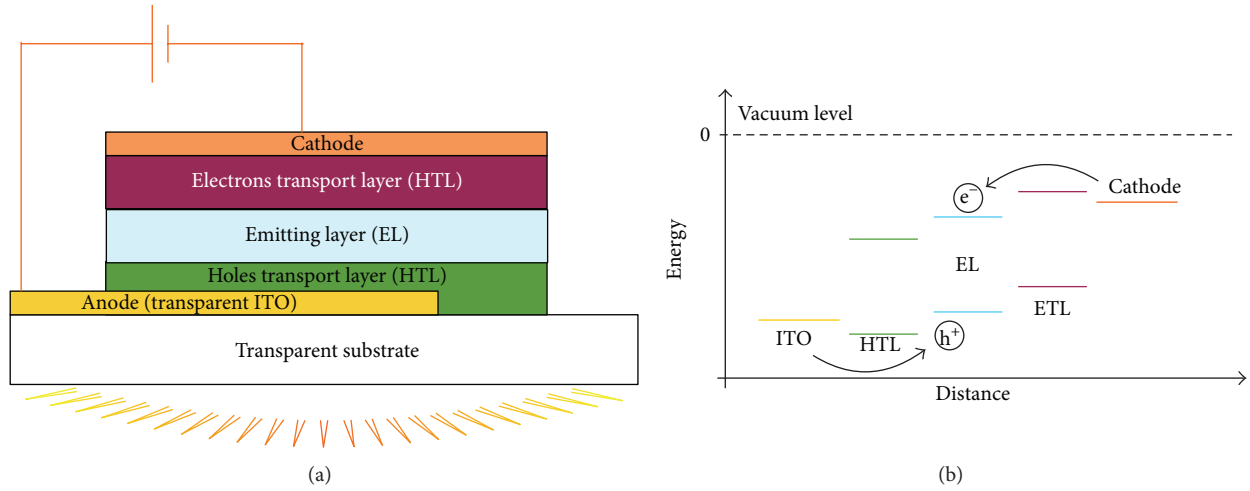

(a) (b)

Figure 14: (a) Cross-section of a typical OLED structure. Hole and electrons are injected from the electrodes into the active layer, where they recombine. The light (here shown as a yellow to orange band) is emitted from the transparent substrate. (b) Scheme of the electrons levels (versus the vacuum level). An ambipolar injection mechanism is required to maximize the device efficiency.

levels is fundamental to avoid the formation of large energetic barriers and prevent the recombination within the active area. Currently OLEDs with external quantum efficiency higher than 50% were reported [169, 170] and external quantum efficiencies of the order of 20% were recently demonstrated in both green [171, 172] and blue [173, 174] OLEDs. The efficiency of the OLED is strongly bound to the dynamics of the recombination of the exciton formed upon excitation. In particular the high probability of having intersystem crossing and the subsequent formation of triplet states may pose a serious limit to the maximum efficiency attainable [175–177]. Reduced lifetime was one of the weakest points of these materials in the early days of their development. Nowadays lifetime in the order of hundreds of thousands of hours is achieved [178]. This value is compatible with market requirements as it is demonstrated by the commercialization of OLED-based display by several companies worldwide. The main advantages of organics compared to LCD technology are the larger viewing angles, higher contrast, and lower power consumption.

Another widely investigated structure is the organic field effect transistor (OFET) and the organic light emitting transistor (OLET). FETs are a fundamental building block of the modern electronic era and the basic properties of organic based FET are discussed in detail in several monographs [152, 179]. Compared to OLEDs, OLETs allow for higher current density to be injected and permit the placement of the recombination area far from the electrodes; thus they reduce the losses due to reabsorption of photons by opaque metallic electrodes. Furthermore OFET may find use in field-driven display technology and flexible displays based on these devices were already demonstrated [180, 181]. OFETs were

used to fabricate an artificial skin that exploited the different resistance of the pixels when subjected to mechanical load [182]. Finally OFETs may be used in RFID technology. Their low thermal budget and the possibility to fabricate RFID using printing technology may greatly reduce the cost of this technology and widen its use [183, 184].

Despite the fascinating possibilities offered by organic compounds only few works published so far demonstrated the possibility to couple OLEDs with WGs to fabricate an integrated optical circuit. The first demonstration of an OLED coupled to a waveguide was presented by Ohmori et al. [185, 186]. The coupling was achieved by cutting a WG facet at 45°C to bend the light output from the OLED and couple it to the WG. Coupling efficiency was limited because of a poorly optimized out-of-plane light coupling, but the authors were able to demonstrate video transmission using this system. After this proof-of-principle demonstration only few other works focused on this integration [187, 188] and although a number of active and passive elements were already fabricated using organic materials, the realization of the first optical circuit based on organic materials has not yet been demonstrated.

6. Sol-Gel

The sol-gel process was developed several decades ago as chemical synthesis to produce ceramics and glass using a low-temperature method. Due to its flexibility the method became soon popular and there is extensive bibliography that describes it in detail [189, 190]. The sol-gel process can be roughly described as a polymerization reaction that starts from (organometallic) molecular precursors to obtain bulk—but also thin film—glass. The molecular precursor undergoes (catalyzed) hydrolysis and condensation reactions to form a three-dimensional network. Due to its very general mechanism of reaction sol-gel is used to synthesize single and multicomponent glass and it permits a fine tuning of the final composition and of the properties of the glass.

Sol-gel has great potentiality to synthesize functional nanomaterials dispersed into glass matrices with well-know and controlled properties. For example, the sol-gel process was successfully used to nucleate silicon nanocrystals within silica matrix. Different reactions were proposed and they all considered the use of silane precursor that after polymerization gave rise to the formation of a nonstoichiometric silica glass containing an excess of silicon atoms. An annealing treatment at temperature above 1100°C allows the silicon atoms to diffuse and to nucleate QDs. Synthetic methods considering TEOS and TREOS precursor permit obtaining both bulk and thin film silica-based materials with rather high concentration of silicon QDs that maintain bright luminescence under optical excitation [191, 192].

Figure 15(a) shows bulk samples produced from TREOS-based synthesis. The pink color of the left sample is due to the Erbium ions that were introduced into the glass, while the dark color of the samples on the right is related to the formation of carbon residues after the pyrolysis, because of a noncomplete hydrolysis during the gelification process.

Recently similar materials were synthesized starting from tetrachlorosilane [193]. Compared to the previously mentioned method, its main advantage relies on the absence of carbon in the precursor. The glass shows higher transparency because no carbonaceous residuals are present after the thermal treatment.

The emission peak of glass obtained from this receipt is shown in Figure 15(b). Emission wavelength can be tuned by changing the synthesis conditions (such as reaction time, atmosphere composition, and annealing temperature). Despite the presence of carbon impurities that increase the absorption in the visible part of the spectrum, sol-gel synthesis of silicon-oxycarbide glass (which uses precursors that contain carbon atoms) is of interest because of their broad photoluminescence peak that can be exploited to fabricate white emitting light source [194].

Compared to the fabrication of silicon QDs starting from porous silicon samples, the sol-gel synthesis is a simpler, cleaner, and more effective way to synthesize large quantity of nanoparticles with controlled structure and surface state. The QDs size dispersion can be controlled to a higher extent and because the nanoparticles are neither exposed to air nor to solvents, their surface state has better reproducibility that is reflected on more homogeneous optoelectronic properties.

Sol-gel thin film can be patterned with standard lithographic techniques. The film may contain photoreactive dye that increases the film solubility upon being exposed to the desired lithographic source (UV-vis, electron, or X-ray beam). Otherwise the desired pattern can be transferred to the thin film by patterning a commercial photoresist and then etching the underlying sol-gel layer (as shown Figure 16).

Below the most recent results obtained using sol-gel glass to fabricate integrated photonics devices are resumed.

Despite its great potentialities sol-gel has found limited uses in the development of integrated photonics. This is because, as for all the liquid based synthesis of ceramic materials, it is extremely difficult to control the shrinkage during the densification step that reduces the dimension of the material and prevent a precise control over the final size. Moreover it is hard to synthesize functional glass of optical quality with perfectly homogeneous refractive index and being cracks free. Thus, up to now, the sol-gel method has been used to fabricate thin films that are subsequently processed using different types of lithographic processes such as standard photolithography [195–198], two-photon laser processing [199], and soft imprinting [200]. A recent review of the results achieved so far is in [201].

Despite the aforementioned fundamental limits, sol-gel based materials have intriguing possibilities due to the large tunability of their properties and the possibility to be functionalized with a large number of optically active molecular compounds. The advancements in the fabrication technologies have recently permit demonstrating that sol-gel based materials can be integrated in a planar optical circuit to fabricate high-performance electrooptic modulators [202, 203]. These results open the way for future implementation

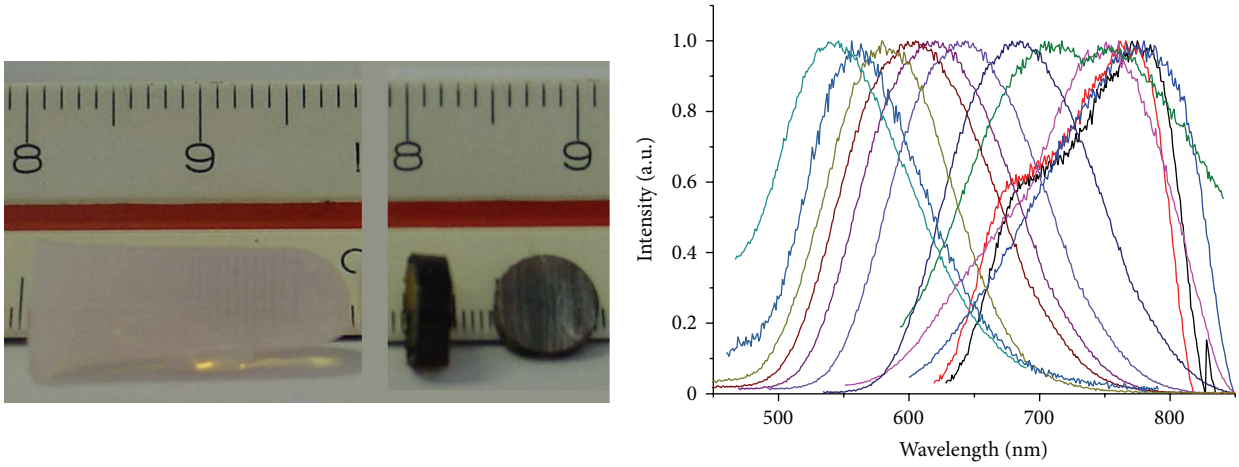

Figure 15: (a) Sol-gel glass synthesized from TREOS precursors. On the left: a bulk sample before the annealing process. The pink color is due to the doping of the glass with Erbium ions. On the right: two slices of glass after the pyrolysis. The dark color is due to carbon residuals (scale is in mm). (b) Photoluminescence of sol-gel silica containing silicon QDs obtained from tetrachlorosilane. The peak emission wavelength can be tuned over most of the visible spectrum by proper tuning of the synthesis conditions.

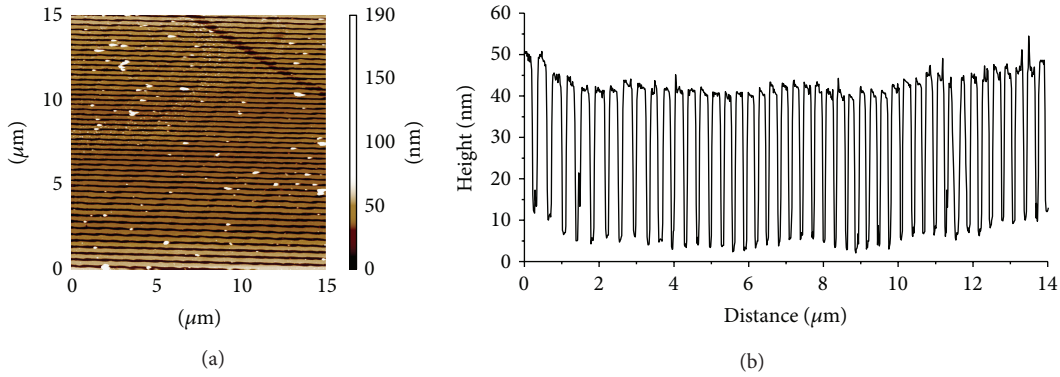

Figure 16: Example of nanostructures transferred into a sol-gel thin layer. The pattern was created using electron-beam lithography into a commercial resist. After the development of the resist, the pattern was transferred into the sol-gel glass. (a) AFM map of a patterned area. (b) Height profile. The lattice pitch of the one-dimensional grating inscribed is of 200 nm.

of functional devices prepared using the sol-gel technology in photonic integrated circuits.

7. Conclusions and Future Perspectives

Integrated photonics is a key enabling technology that will pave the way for the conception and development of radically innovative devices. It will surely drive the evolution of information and communication technologies for the next decades and here the major role will be played by inorganic materials (both silicon and III/V or II/VI based). Their optical, electrical, and mechanical properties render them the ideal dielectrics in which optoelectronic circuits are realized with a high level of device integration. Still the integration of organic materials enables the addiction of novel and more complex functionalities that are difficult (if not impossible) to achieve using a purely inorganic framework. Organics have important advantages in terms of flexibility and tunability of their properties. Their molecular structure and the bottom-up synthetic approaches that are often used to prepare them permit a fine tailoring of their properties to exactly fulfill the requirements needed by the application they have to be used in. Their weaknesses (such as thermal and mechanical stability) are constantly improved and several products have already reached the market (like organic displays and screens exploiting III/V QDs). Some examples of both active and passive devices recently fabricated using such hybrid approach were presented in this review but several other approaches were so far proposed and may result in clever technological solutions (e.g., optofluidics is gaining interest for the possibility of realizing highly reconfigurable systems [204, 205]).

But the realm of the hybrid photonics goes well beyond the applications in communication systems. The advancement in nanotechnologies is opening the fascinating possibility to couple monitoring and sensing elements directly

with living organisms. This fact will be a breakthrough for health care systems because biophotonics allows the fabrication of real time, point of care, and minimally invasive screening methods. These technologies will provide a risk assessment of life style and age related diseases and thus offer a personalized and constantly updated diagnosis. Among the examples recently proposed in literature the biodegradable (sometime also called *transient*) electronics [206, 207] and the silk [208, 209] based photonics are the most promising ones. The former topic suggests the possibility to use organics to fabricate optoelectronics circuits that can be implanted (or edible) and that perform their action of monitoring or drug releasing for a controlled period of time within the host body. The latter proposes the fabrication of photonic devices made of silk. Silk is a very robust and transparent fiber that is easily (nano)structured to give it photonic functionalities.

These two unconventional approaches to hybrid photonics are probably the tip of a still unknown iceberg that will emerge in the coming years. A truly multidisciplinary research approach, where all the aspects of such complex interacting systems have to be considered and fully understood, is required to fully exploit the potential of this new branch of applied science.

Conflict of Interests

The author declares that there is no conflict of interests regarding the publication of this paper.

Acknowledgments

The author gratefully acknowledges all the colleagues and collaborators for their valuable support, in particular Dr. Romain Guider and Dr. Tullio Toccoli for the data provided.

References

[1] I. Weir, G. Archenhold, M. Robinson, M. Williams, and P. Hilton, "Photonics Technologies and market for a low carbon economy," Summary report published by EC, (Paderborn), 2012.

[2] C. Kachris, K. Bergman, and I. Tomkos, Eds., *Optical Interconnects for Future Data Center Networks*, Springer, New York, NY, USA, 2013.

[3] A. V. Krishnamoorthy, "Progress in low-power switched optical interconnects," *IEEE Journal of Selected Topics in Quantum Electronics*, vol. 17, no. 2, pp. 357–376, 2011.

[4] C. Mesaritakis, V. Papataxiarhis, and D. Syvridis, "Microring resonators as building blocks for an all-optical high-speed reservoir-computing bit-pattern-recognition system," *Journal of Optical Society of America B: Optical Physics*, vol. 30, no. 11, pp. 3048–3055, 2013.

[5] D. Brunner, M. Cornelles Soriano, and I. Fischer, "High-speed optical vector and matrix operations using a semiconductor laser," *IEEE Photonics Technology Letters*, vol. 25, no. 17, pp. 1680–1683, 2013.

[6] D. Brunner, M. C. Soriano, C. R. Mirasso, and I. Fischer, "Parallel photonic information processing at gigabyte per second data rates using transient states," *Nature Communications*, vol. 4, p. 1364, 2013.

[7] M. C. Soriano, J. García-Ojalvo, C. R. Mirasso, and I. Fischer, "Complex photonics: dynamics and applications of delay-coupled semiconductors lasers," *Reviews of Modern Physics*, vol. 85, no. 1, pp. 421–470, 2013.

[8] J. Andréasson, U. Pischel, S. D. Straight, T. A. Moore, A. L. Moore, and D. Gust, "All-photonic multifunctional molecular logic device," *Journal of the American Chemical Society*, vol. 133, no. 30, pp. 11641–11648, 2011.

[9] B. Fresch, D. Hiluf, E. Collini, R. D. Levine, and F. Remacl, "Molecular decision trees realized by ultrafast electronic spectroscopy," *Proceedings of the National Academy of Science*, vol. 110, no. 43, pp. 17183–17188, 2013.

[10] O. Wada, "Recent progress in semiconductor-based photonic signal-processing devices," *IEEE Journal on Selected Topics in Quantum Electronics*, vol. 17, no. 2, pp. 309–319, 2011.

[11] M. Fiorani, M. Casoni, and S. Aleksic, "Hybrid optical switching for an energy-efficient internet core," *IEEE Internet Computing*, vol. 17, no. 1, pp. 14–22, 2013.

[12] G. Cook and J. van Horn, "How dirt is your data?" Greenpeace International, 2011, http://www.greenpeace.org/international/Global/international/publications/climate/2011/Cool%20IT/dirty-data-report-greenpeace.pdf.

[13] G. Lifante, *Integrated Photonics: Fundamentals*, Wiley, 2003.

[14] R. Nagarajan and M. Smit, "Photonic integration," *IEEE LEOS Newsletter*, pp. 4–10, 2007.

[15] Y. J. Heo and S. Takeuchi, "Towards smart tattoos: implantable biosensors for continuous glucose monitoring," *Advanced Healthcare Materials*, vol. 2, no. 1, pp. 43–56, 2013.

[16] T. B. Singh, N. S. Sariciftci, and J. G. Grote, "Bio-organic optoelectronic devices using DNA," in *Organic Electronics*, vol. 223 of *Advances in Polymer Science*, pp. 73–112, Springer, 2010.

[17] D.-H. Kim, R. Ghaffari, N. Lu, and J. A. Rogers, "Flexible and stretchable electronics for biointegrated devices," *Annual Review of Biomedical Engineering*, vol. 14, pp. 113–128, 2012.

[18] H. Ko, R. Kapadia, K. Takei, T. Takahashi, X. Zhang, and A. Javey, "Multifunctional, flexible electronic systems based on engineered nanostructured materials," *Nanotechnology*, vol. 23, no. 34, Article ID 344001, 2012.

[19] M. Singh, H. M. Haverinen, P. Dhagat, and G. E. Jabbour, "Inkjet printing-process and its applications," *Advanced Materials*, vol. 22, no. 6, pp. 673–685, 2010.

[20] M. Jung, J. Kim, J. Noh et al., "All-Printed and roll-to-roll-printable 13.56-MHz-operated 1-bit RF tag on plastic foils," *IEEE Transactions on Electron Devices*, vol. 57, no. 3, pp. 571–580, 2010.

[21] D. Briand, A. Oprea, J. Courbat, and N. Bârsan, "Making environmental sensors on plastic foil," *Materials Today*, vol. 14, no. 9, pp. 416–423, 2011.

[22] P. F. Moonen, I. Yakimets, and J. Huskens, "Fabrication of transistors on flexible substrates: from mass-printing to high-resolution alternative lithography strategies," *Advanced Materials*, vol. 24, no. 41, pp. 5526–5541, 2012.

[23] M. J. R. Heck, M. L. Davenport, and J. E. Bowers, "Progress in hybrid-silicon photonic integrated circuit technology," *SPIE Newsroom*, 2013.

[24] D. Liang and J. E. Bowers, "Recent progress in lasers on silicon," *Nature Photonics*, vol. 4, no. 8, pp. 511–517, 2010.

[25] G. Roelkens, Y. D. Koninck, S. Keyvaninia et al., "Hybrid silicon lasers," in *Optoelectronic Integrated Circuits XIII*, L. A. Eldada and E.-H. Lee, Eds., vol. 7972 of *Proceedings of SPIE*, January 2011.

[26] A. W. Fang, H. Park, Y.-H. Kuo et al., "Hybrid silicon evanescent devices," *Materials Today*, vol. 10, no. 7-8, pp. 28–35, 2007.

[27] G. Roelkens, L. Liu, D. Liang et al., "III-V/silicon photonics for on-chip and intra-chip optical interconnects," *Laser & Photonics Reviews*, vol. 4, no. 6, pp. 751–779, 2010.

[28] J. van Campenhout, L. Liu, P. R. Romeo et al., "A compact SOI-integrated multiwavelength laser source based on cascaded InP microdisks," *IEEE Photonics Technology Letters*, vol. 20, no. 16, pp. 1345–1347, 2008.

[29] M. Lamponi, S. Keyvaninia, C. Jany et al., "Heterogeneously integrated InP/SOI laser using double tapered single-mode waveguides through adhesive die to wafer bonding," in *Proceedings of the 7th IEEE International Conference on Group IV Photonics (GFP '10)*, pp. 22–24, Beijing, China, September 2010.

[30] S. Keyvaninia, G. Roelkens, D. van Thourhout et al., "Demonstration of a heterogeneously integrated III-V/SOI single wavelength tunable laser," *Optics Express*, vol. 21, no. 3, pp. 3784–3792, 2013.

[31] S. Keyvaninia, G. Roelkens, R. Baets et al., "Demonstration of a novel III-V-on-Si distributed feedback laser," in *Proceedings of the Optical Fiber Communication Conference and Exposition and the National Fiber Optic Engineers Conference (OFC/NFOEC '13)*, 2013.

[32] Z. Huang and Y. Wang, "Four-wavelength III-V/SOI heterogeneous integrated laser based on sampled bragg grating for CWDM," *IEEE Photonics Journal*, vol. 5, no. 5, Article ID 1501906, 2013.

[33] V. I. Klimov, A. A. Mikhailovsky, S. Xu et al., "Optical gain and stimulated emission in nanocrystal quantum dots," *Science*, vol. 290, no. 5490, pp. 314–317, 2000.

[34] M. S. Bakshi, P. Thakur, G. Kaur et al., "Stabilization of PbS nanocrystals by bovine serum albumin in its native and denatured states," *Advanced Functional Materials*, vol. 19, no. 9, pp. 1451–1458, 2009.

[35] A. Omari, I. Moreels, F. Masia et al., "Role of interband and photoinduced absorption in the nonlinear refraction and absorption of resonantly excited PbS quantum dots around 1550 nm," *Physical Review B: Condensed Matter and Materials Physics*, vol. 85, no. 11, Article ID 115318, 2012.

[36] Y. K. Olsson, G. Chen, R. Rapaport et al., "Fabrication and optical properties of polymeric waveguides containing nanocrystalline quantum dots," *Applied Physics Letters*, vol. 85, no. 19, pp. 4469–4471, 2004.

[37] J. Grandidier, G. C. des Francs, S. Massenot et al., "Gain-assisted propagation in a plasmonic waveguide at telecom wavelength," *Nano Letters*, vol. 9, no. 8, pp. 2935–2939, 2009.

[38] N. Tessler, V. Medvedev, M. Kazes, S. Kan, and U. Banin, "Efficient near-infrared polymer nanocrystal light-emitting diodes," *Science*, vol. 295, no. 5559, pp. 1506–1508, 2002.

[39] L. Bakueva, S. Musikhin, M. A. Hines et al., "Size-tunable infrared (1000-1600 nm) electroluminescence from PbS quantum-dot nanocrystals in a semiconducting polymer," *Applied Physics Letters*, vol. 82, no. 17, pp. 2895–2897, 2003.

[40] M. Humer, R. Guider, W. Jantsch, and T. Fromherz, "Integration, photostability and spontaneous emission rate enhancement of colloidal PbS nanocrystals for Si-based photonics at telecom wavelengths," *Optics Express*, vol. 21, no. 16, pp. 18680–[18688, 2013.

[41] Y. Shoji, T. Ogasawara, T. Kamei et al., "Ultrafast nonlinear effects in hydrogenated amorphous silicon wire waveguide," *Optics Express*, vol. 18, no. 6, pp. 5668–5673, 2010.

[42] Y. A. Vlasov and S. J. McNab, "Losses in single-mode silicon-on-insulator strip waveguides and bends," *Optics Express*, vol. 12, no. 8, pp. 1622–1631, 2004.

[43] M. Humer, R. Guider, W. Jantsch, and T. Fromherz, "Colloidal PbS nanocrystals integrated to Si-based photonics for applications at telecom wavelengths," in *International Society for Optical Engineering*, J. M. Fedeli, L. Vivien, and M. K. Smit, Eds., vol. 8767 of *Proceedings of SPIE*, 2013.

[44] A. Omari, P. Geiregat, D. van Thourhout, and Z. Hens, "Light absorption in hybrid silicon-on insulator/quantum dot waveguides," *Optics Express*, vol. 21, no. 20, pp. 23272–23285, 2013.

[45] K. A. Abel, J. Shan, J.-C. Boyer, F. Harris, and F. C. J. M. van Veggel, "Highly photoluminescent PbS nanocrystals: The beneficial effects of trioctylphosphine," *Chemistry of Materials*, vol. 20, no. 12, pp. 3794–3796, 2008.

[46] S. M. Geyer, J. M. Scherer, M. G. Bawendi, and F. Jaworski, "Dual Band ultraviolet-short-wavelength imaging via luminescent down-shifting with colloidal quantum dots," *Journal of Nanophotonic*, vol. 7, no. 1, Article ID 073083, 2013.

[47] M. S. Neo, N. Venkatram, G. S. Li, W. S. Chin, and W. Ji, "Synthesis of PbS/CdS core-shell QDs and their nonlinear optical properties," *Journal of Physical Chemistry C*, vol. 114, no. 42, pp. 18037–18044, 2010.

[48] P. J. Landrigan, "Occupational and community exposures to toxic metals: Lead, cadmium, mercury and arsenic," *The Western Journal of Medicine*, vol. 137, no. 6, pp. 531–539, 1982.

[49] S. T. Selvan, T. T. Tan, and J. Y. Ying, "Robust, non-cytotoxic, silica-coated CdSe quantum dots with efficient photoluminescence," *Advanced Materials*, vol. 17, no. 13, pp. 1620–1625, 2005.

[50] R. Han, M. Yu, Q. Zheng, L. Wang, Y. Hong, and Y. Sha, "A facile synthesis of small-sized, highly photoluminescent, and monodisperse CdSeS QD/SiO_2 for live cell imaging," *Langmuir*, vol. 25, no. 20, pp. 12250–12255, 2009.

[51] R. Koole, M. M. van Schooneveld, J. Hilhorst et al., "On the incorporation mechanism of hydrophobic quantum dots in silica spheres by a reverse microemulsion method," *Chemistry of Materials*, vol. 20, no. 7, pp. 2503–2512, 2008.

[52] E. D. Kosten, E. L. Warren, and H. A. Atwater, "Ray optical light trapping in silicon microwires: exceeding the $2n^2$ intensity limit," *Optics Express*, vol. 19, no. 4, pp. 3316–3331, 2011.

[53] S. L. Diedenhofen, O. T. A. Janssen, G. Grzela, E. P. A. M. Bakkers, and J. Gómez Rivas, "Strong geometrical dependence of the absorption of light in arrays of semiconductor nanowires," *ACS Nano*, vol. 5, no. 3, pp. 2316–2323, 2011.

[54] M. Heiss and A. Fontcuberta i Morral, "Fundamental limits in the external quantum efficiency of single nanowire solar cells," *Applied Physics Letters*, vol. 99, no. 26, Article ID 263102, 2011.

[55] D. Milam, "Review and assessment of measured values of the nonlinear refractive-index coefficient of fused silica," *Applied Optics*, vol. 37, no. 3, pp. 546–550, 1998.

[56] M. Dinu, F. Quochi, and H. Garcia, "Third-order nonlinearities in silicon at telecom wavelengths," *Applied Physics Letters*, vol. 82, no. 18, pp. 2954–2956, 2003.

[57] A. Villeneuve, C. C. Yang, G. I. Stegeman, C.-H. Lin, and H.-H. Lin, "Nonlinear refractive-index and two photon-absorption near half the band gap in AlGaAs," *Applied Physics Letters*, vol. 62, no. 20, pp. 2465–2467, 1993.

[58] J. T. Gopinath, M. Soljačić, E. P. Ippen, V. N. Fuflyigin, W. A. King, and M. Shurgalin, "Third order nonlinearities in Ge-As-Se-based glasses for telecommunications applications," *Journal of Applied Physics*, vol. 96, no. 11, pp. 6931–6933, 2004.

[59] T. Vallaitis, S. Bogatscher, L. Alloatti et al., "Optical properties of highly nonlinear silicon-organic hybrid (SQH) waveguide geometries," *Optics Express*, vol. 17, no. 20, pp. 17357–17368, 2009.

[60] P. Krogstrup, H. I. Jørgensen, M. Heiss et al., "Single-nanowire solar cells beyond the Shockley-Queisser limit," *Nature Photonics*, vol. 7, no. 4, pp. 306–310, 2013.

[61] M. Hochberg and T. Baehr-Jones, "Towards fabless silicon photonics," *Nature Photonics*, vol. 4, no. 8, pp. 492–494, 2010.

[62] Z. Zhang, *Silicon-based photonic devices: design, fabrication and characterization [Ph.D. thesis]*, Royal Institute of Technology (KTH), 2008.

[63] C. Wagner and N. Harned, "EUV lithography: lithography gets extreme," *Nature Photonics*, vol. 4, no. 1, pp. 24–26, 2010.

[64] X. Liang, Y.-S. Jung, S. Wu et al., "Formation of bandgap and subbands in graphene nanomeshes with sub-10 nm ribbon width fabricated via nanoimprint lithography," *Nano Letters*, vol. 10, no. 7, pp. 2454–2460, 2010.

[65] V. R. Manfrinato, L. Zhang, D. Su et al., "Resolution limits of electron-beam lithography toward the atomic scale," *Nano Letters*, vol. 13, no. 4, pp. 1555–1558, 2013.

[66] J. Leuthold, W. Freude, J.-M. Brosi et al., "Silicon organic hybrid technology—a platform for practical nonlinear optics," *Proceedings of the IEEE*, vol. 97, no. 7, pp. 1304–1315, 2009.

[67] M. Lipson, "Guiding, modulating, and emitting light on silicon—challenges and opportunities," *Journal of Lightwave Technology*, vol. 23, no. 12, pp. 4222–4238, 2005.

[68] M. J. R. Heck, J. F. Bauters, M. L. Davenport et al., "Hybrid silicon photonic integrated circuit technology," *IEEE Journal on Selected Topics in Quantum Electronics*, vol. 19, no. 4, Article ID 6100117, 2013.

[69] S. Jeong, E. C. Garnett, S. Wang et al., "Hybrid silicon nanocone-polymer solar cells," *Nano Letters*, vol. 12, no. 6, pp. 2971–2976, 2012.

[70] C. Kopp, S. Bernabé, B. B. Bakir et al., "Silicon photonic circuits: on-CMOS integration, fiber optical coupling, and packaging," *IEEE Journal on Selected Topics in Quantum Electronics*, vol. 17, no. 3, pp. 498–509, 2011.

[71] D. Liang, G. Roelkens, R. Baets, and J. E. Bowers, "Hybrid integrated platforms for silicon photonics," *Materials*, vol. 3, no. 3, pp. 1782–1802, 2010.

[72] T. Hong, G.-Z. Ran, T. Chen et al., "A selective-area metal bonding InGaAsP-Si laser," *IEEE Photonics Technology Letters*, vol. 22, no. 15, pp. 1141–1143, 2010.

[73] J. Justice, C. Bower, M. Meitl, M. B. Mooney, M. A. Gubbins, and B. Corbett, "Wafer-scale integration of group III-V lasers on silicon using transfer printing of epitaxial layers," *Nature Photonics*, vol. 6, no. 9, pp. 610–614, 2012.

[74] Y. Justo, I. Moreels, K. Lambert, and Z. Hens, "Langmuir-Blodgett monolayers of colloidal lead chalcogenide quantum dots: Morphology and photoluminescence," *Nanotechnology*, vol. 21, no. 29, Article ID 295606, 2010.

[75] C. Ingrosso, V. Fakhfouri, M. Striccoli et al., "An epoxy photoresist modified by luminescent nanocrystals for the fabrication of 3D high-aspect-ratio microstructures," *Advanced Functional Materials*, vol. 17, no. 13, pp. 2009–2017, 2007.

[76] M. Wang, *Lithography*, InTech, 2010.

[77] K. S. Novoselov, A. K. Geim, S. V. Morozov et al., "Electric field in atomically thin carbon films," *Science*, vol. 306, no. 5696, pp. 666–669, 2004.

[78] R. R. Nair, P. Blake, A. N. Grigorenko et al., "Fine structure constant defines visual transparency of graphene," *Science*, vol. 320, no. 5881, p. 1308, 2008.

[79] K. Kim, J.-Y. Choi, T. Kim, S.-H. Cho, and H.-J. Chung, "A role for graphene in silicon-based semiconductor devices," *Nature*, vol. 479, no. 7373, pp. 338–344, 2011.

[80] S. D. Sarma, S. Adam, E. H. Hwang, and E. Rossi, "Electronic transport in two-dimensional graphene," *Reviews of Modern Physics*, vol. 83, no. 2, pp. 407–470, 2011.

[81] T. Palacios, "Graphene electronics: thinking outside the silicon box," *Nature Nanotechnology*, vol. 6, no. 8, pp. 464–465, 2011.

[82] E. Hendry, P. J. Hale, J. Moger, A. K. Savchenko, and S. A. Mikhailov, "Coherent nonlinear optical response of graphene," *Physical Review Letters*, vol. 105, no. 9, Article ID 097401, 2010.

[83] R. Won, "Photovoltaics: graphene-silicon solar cells," *Nature Photonics*, vol. 4, no. 7, p. 411, 2010.

[84] L. Oakes, A. Westover, J. W. Mares et al., "Surface engineered porous silicon for stable, high performance electrochemical supercapacitors," *Scientific Reports*, vol. 3, p. 3020, 2013.

[85] M. Liu and X. Zhang, "Silicon photonics: graphene benefits," *Nature Photonics*, vol. 7, pp. 851–852, 2013.

[86] X. Gan, R. J. Shiue, Y. Gao et al., "Chip-integrated ultrafast graphene photodetector with high responsivity," *Nature Photonics*, vol. 7, no. 11, pp. 883–887, 2013.

[87] A. Pospischil, M. Humer, M. M. Furchi et al., "CMOS-compatible graphene photodetector covering all optical communication bands," *Nature Photonics*, vol. 7, no. 11, pp. 892–896, 2013.

[88] X. Wang, Z. Cheng, K. Xu, H. K. Tsang, and J. B. Xu, "High-responsivity graphene/silicon-heterostructure waveguide photodetectors," *Nature Photonics*, vol. 7, no. 11, pp. 888–891, 2013.

[89] F. Xia, T. Mueller, Y.-M. Lin, A. Valdes-Garcia, and P. Avouris, "Ultrafast graphene photodetector," *Nature Nanotechnology*, vol. 4, no. 12, pp. 839–843, 2009.

[90] S. Y. Hong, J. I. Dadap, N. Petrone, P. C. Yeh, J. Hone, and R. M. Osgood Jr., "Optical third-harmonic generation in graphene," *Physical Review*, vol. 3, Article ID 021014, 2013.

[91] T. Gu, N. Petrone, J. F. McMillan et al., "Regenerative oscillation and four-wave mixing in graphene optoelectronics," *Nature Photonics*, vol. 6, no. 8, pp. 554–559, 2012.

[92] A. Pasquazi, M. Peccianti, Y. Park et al., "Sub-picosecond phase-sensitive optical pulse characterization on a chip," *Nature Photonics*, vol. 5, no. 10, pp. 618–623, 2011.

[93] F. Wang, Y. Zhang, C. Tian et al., "Gate-variable optical transitions in graphene," *Science*, vol. 320, no. 5873, pp. 206–209, 2008.

[94] A. Majumdar, J. Kim, J. Vuckovic, and F. Wang, "Electrical control of silicon photonic crystal cavity by graphene," *Nano Letters*, vol. 13, no. 2, pp. 515–518, 2013.

[95] Y. Jia, J. Wei, K. Wang et al., "Nanotube-silicon heterojunction solar cells," *Advanced Materials*, vol. 20, no. 23, pp. 4594–4598, 2008.

[96] A. Arena, N. Donato, G. Saitta, S. Galvagno, C. Milone, and A. Pistone, "Photovoltaic properties of multi-walled carbon nanotubes deposited on n-doped silicon," *Microelectronics Journal*, vol. 39, no. 12, pp. 1659–1662, 2008.

[97] Y. Jung, X. Li, N. K. Rajan, A. D. Taylor, and M. A. Reed, "Record high efficiency single-walled carbon nanotube/silicon p-n junction solar cells," *Nano Letters*, vol. 13, no. 1, pp. 95–99, 2013.

[98] X. Li, H. Zhu, K. Wang et al., "Graphene-on-silicon schottky junction solar cells," *Advanced Materials*, vol. 22, no. 25, pp. 2743–2748, 2010.

[99] M. A. Green, K. Emery, Y. Hishikawa, W. Warta, and E. D. Dunlop, "Solar cell efficiency tables (version 39)," *Progress in Photovoltaics: Research and Applications*, vol. 20, no. 1, pp. 12–20, 2012.

[100] A. Jane, R. Dronov, A. Hodges, and N. H. Voelcker, "Porous silicon biosensors on the advance," *Trends in Biotechnology*, vol. 27, no. 4, pp. 230–239, 2009.

[101] N. Kumar, S. Gennaro, P. V. W. Sasikumar, G. D. Soraru, and P. Bettotti, "Self detachment of free-standing porous silicon membranes in moderately doped n-type silicon," *Applied Physics A*, 2013.

[102] L. Eldada and L. W. Shacklette, "Advances in polymer integrated optics," *IEEE Journal on Selected Topics in Quantum Electronics*, vol. 6, no. 1, pp. 54–68, 2000.

[103] H. Ma, A. K. Y. Jen, and L. R. Dalton, "Polymer-based optical waveguides: materials, processing, and devices," *Advanced Materials*, vol. 14, no. 9, pp. 1339–1365, 2002.

[104] Z. Zhang, N. Mettbach, C. Zawadzki et al., "Polymer-based photonic toolbox: passive components, hybrid integration and polarisation control," *IET Optoelectronics*, vol. 5, no. 5, pp. 226–232, 2011.

[105] M.-C. Oh, K.-J. Kim, W.-S. Chu et al., "Integrated photonic devices incorporating low-loss fluorinated polymer materials," *Polymers*, vol. 3, no. 3, pp. 975–997, 2011.

[106] J.-G. Liu and M. Ueda, "High refractive index polymers: fundamental research and practical applications," *Journal of Materials Chemistry*, vol. 19, no. 47, pp. 8907–8919, 2009.

[107] A. Zebda, L. Camberlein, B. Bêche et al., "Spin coating and plasma process for 2.5D integrated photonics on multilayer polymers," *Thin Solid Films*, vol. 516, no. 23, pp. 8668–8674, 2008.

[108] M. Nordström, D. A. Zauner, A. Boisen, and J. Hübner, "Single-mode waveguides with SU-8 polymer core and cladding for MOEMS applications," *Journal of Lightwave Technology*, vol. 25, no. 5, pp. 1284–1289, 2007.

[109] S.-W. Ahn, K.-D. Lee, D.-H. Kim, and S.-S. Lee, "Polymeric wavelength filter based on a Bragg grating using nanoimprint technique," *IEEE Photonics Technology Letters*, vol. 17, no. 10, pp. 2122–2124, 2005.

[110] R. Kirchner, M.-K. Kaiser, B. Adolphi, R. Landgraf, and W.-J. Fischer, "Chemical functional polymers for direct UV assisted nanoimprinting of polymeric photonic microring resonators," *Physica Status Solidi A*, vol. 208, no. 6, pp. 1308–1314, 2011.

[111] L. Li, E. Gershgoren, G. Kumi et al., "High-performance microring resonators fabricated with multiphoton absorption polymerization," *Advanced Materials*, vol. 20, no. 19, pp. 3668–3671, 2008.

[112] J. Luo and A. K. Y. Jen, "Highly efficient organic electrooptic materials and their hybrid systems for advanced photonic devices," *IEEE Journal of Selected Topics in Quantum Electronics*, vol. 19, no. 6, Article ID 3401012, 2013.

[113] L. Yin and G. P. Agrawal, "Impact of two-photon absorption on self-phase modulation in silicon waveguides," *Optics Letters*, vol. 32, no. 14, pp. 2031–2033, 2007.

[114] A. D. Bristow, N. Rotenberg, and H. M. van Driel, "Two-photon absorption and Kerr coefficients of silicon for 850-2200 nm," *Applied Physics Letters*, vol. 90, no. 19, Article ID 191104, 2007.

[115] M.-C. Oh, H. Zhang, A. Szep et al., "Electro-optic polymer modulators for 1.55 μm wavelength using phenyltetraene bridged chromophore in polycarbonate," *Applied Physics Letters*, vol. 76, no. 24, pp. 3525–3527, 2000.

[116] G. Yu, J. Mallari, H. Shen et al., "40GHz zero chirp single-ended EO polymer modulators with low half-wave voltage," in *Proceedings of the Conference on Lasers and Electro-Optics (CLEO '11)*, Baltimore, Md, USA, May 2011.

[117] X. Zhang, A. Hosseini, X. Lin, H. Subbaraman, and R. T. Chen, "Polymer-based hybrid-integrated photonic devices for silicon on-chip modulation and board-level optical interconnects," *IEEE Journal of Selected Topics in Quantum Electronics*, vol. 19, no. 6, Article ID 3401115, 2013.

[118] R. Dinu, D. Jin, G. Yu et al., "Environmental stress testing of electro-optic polymer modulators," *Journal of Lightwave Technology*, vol. 27, no. 11, pp. 1527–1532, 2009.

[119] D. Jin, H. Chen, A. Barklund et al., "EO polymer modulators reliability study," in *Organic Photonic Materials and Devices XII*, R. L. Nelson, F. Kajzar, and T. Kaino, Eds., vol. 7599 of *Proceedings of SPIE*, January 2010.

[120] J. Luo, S. Huang, Z. Shi, B. M. Polishak, X.-H. Zhou, and A. K.-Y. Jen, "Tailored organic electro-optic materials and their hybrid systems for device applications," *Chemistry of Materials*, vol. 23, no. 3, pp. 544–553, 2011.

[121] C.-Y. Lin, X. Wang, S. Chakravarty et al., "Electro-optic polymer infiltrated silicon photonic crystal slot waveguide modulator with 23 dB slow light enhancement," *Applied Physics Letters*, vol. 97, no. 9, Article ID 093304, 2010.

[122] C. Koos, P. Vorreau, T. Vallaitis et al., "All-optical high-speed signal processing with silicon-organic hybrid slot waveguides," *Nature Photonics*, vol. 3, no. 4, pp. 216–219, 2009.

[123] S. Inoue and A. Otomo, "Electro-optic polymer/silicon hybrid slow light modulator based on one-dimensional photonic crystal waveguides," *Applied Physics Letters*, vol. 103, no. 17, Article ID 171101, 2013.

[124] J. Leuthold, C. Koos, W. Freude et al., "Silicon-organic hybrid electro-optical devices," *IEEE Journal of Selected Topics in Quantum Electronics*, vol. 19, no. 6, Article ID 3401413, 2013.

[125] V. R. Almeida, Q. Xu, C. A. Barrios, and M. Lipson, "Guiding and confining light in void nanostructure," *Optics Letters*, vol. 29, no. 11, pp. 1209–1211, 2004.

[126] J. T. Robinson, K. Preston, O. Painter, and M. Lipson, "First-principle derivation of gain in high-index-contrast waveguides," *Optics Express*, vol. 16, no. 21, pp. 16659–16669, 2008.

[127] P. Bettotti, A. Pitanti, E. Rigo, F. de Leonardis, V. M. N. Passaro, and L. Pavesi, "Modeling of slot waveguide sensors based on polymeric materials," *Sensors*, vol. 11, no. 8, pp. 7327–7340, 2011.

[128] L. Alloatti, D. Korn, R. Palmer et al., "7 Gbit/s electro-optic modulator in silicon technology," *Optics Express*, vol. 19, no. 12, pp. 11841–11851, 2011.

[129] J.-M. Brosi, C. Koos, L. C. Andreani, M. Waldow, J. Leuthold, and W. Freude, "High-speed low-voltage electro-optic modulator with a polymer-infiltrated silicon photonic crystal waveguide," *Optics Express*, vol. 16, no. 6, pp. 4177–4191, 2008.

[130] I. A. Young, E. Mohammed, J. T. S. Liao et al., "Optical I/O technology for tera-scale computing," *IEEE Journal of Solid-State Circuits*, vol. 45, no. 1, pp. 235–248, 2010.

[131] R. Palmer, L. Alloatti, D. Korn et al., "Low-loss silicon strip-to-slot mode converters," *IEEE Photonics Journal*, vol. 5, no. 1, pp. 1226–1229, 2013.

[132] Y.-O. Noh, C.-H. Lee, J.-M. Kim et al., "Polymer waveguide variable optical attenuator and its reliability," *Optics Communications*, vol. 242, no. 4–6, pp. 533–540, 2004.

[133] S.-H. Park, J.-W. Kim, M.-C. Oh, Y.-O. Noh, and H.-J. Lee, "Polymer waveguide birefringence modulators," *IEEE Photonics Technology Letters*, vol. 24, no. 10, pp. 845–847, 2012.

[134] V. Raghunathan, J. L. Yagüe, J. Xu, J. Michel, K. K. Gleason, and L. C. Kimerling, "Co-polymer clad design for high performance athermal photonic circuits," *Optics Express*, vol. 20, no. 19, pp. 20808–20813, 2012.

[135] Y. Kokubun, S. Yoneda, and H. Tanaka, "Temperature-independent narrowband optical filter at 1.31 μm wavelength by an athermal waveguide," *Electronics Letters*, vol. 32, no. 21, pp. 1998–2000, 1996.

[136] J.-M. Lee, D.-J. Kim, H. Ahn, S.-H. Park, and G. Kim, "Temperature dependence of silicon nanophotonic ring resonator with a polymeric overlayer," *Journal of Lightwave Technology*, vol. 25, no. 8, pp. 2236–2243, 2007.

[137] J.-M. Lee, D.-J. Kim, G.-H. Kim, O.-K. Kwon, K.-J. Kim, and G. Kim, "Controlling temperature dependence of silicon waveguide using slot structure," *Optics Express*, vol. 16, no. 3, pp. 1645–1652, 2008.

[138] J. Teng, P. Dumon, W. Bogaerts et al., "Athermal Silicon-on-insulator ring resonators by overlaying a polymer cladding on narrowed waveguides," *Optics Express*, vol. 17, no. 17, pp. 14627–14633, 2009.

[139] J. Pfeifle, L. Alloatti, W. Freude, J. Leuthold, and C. Koos, "Silicon-organic hybrid phase shifter based on a slot waveguide with a liquid-crystal cladding," *Optics Express*, vol. 20, no. 14, pp. 15359–15376, 2012.

[140] S. Yokoyama, F. Qiu, Y. Feng, A. M. Spring, and K. Yamamoto, "0. 018pm/°C athermal silicon nitride ring resonator by polymer cladding," in *Proceedings of the Conference on Lasers and Electro-Optics Pacific Rim (CLEO-PR '13)*, Kyoto, Japan, 2013.

[141] V. Raghunathan, T. Izuhara, J. Michel, and L. Kimerling, "Stability of polymer-dielectric bi-layers for athermal silicon photonics," *Optics Express*, vol. 20, no. 14, pp. 16059–16066, 2012.

[142] K. S. Hsu, T. T. Chiu, P. T. Lee, and M. H. Shih, "Wavelength tuning by bending a flexible photonic crystal laser," *Journal of Lightwave Technology*, vol. 31, no. 12, pp. 1960–1964, 2013.

[143] Y.-O. Noh, H.-J. Lee, N. J. Ju, M.-S. Kim, S. H. Oh, and M.-C. Oh, "Continuously tunable compact lasers based on thermo-optic polymer waveguides with Bragg gratings," *Optics Express*, vol. 16, no. 22, pp. 18194–18195, 2008.

[144] K.-J. Kim, J.-W. Kim, M.-C. Oh, Y.-O. Noh, and H.-J. Lee, "Flexible polymer waveguide tunable lasers," *Optics Express*, vol. 18, no. 8, pp. 8392–8399, 2010.

[145] F. Ebisawa, T. Kurokawa, and S. Nara, "Electrical properties of polyacetylene/polysiloxane interface," *Journal of Applied Physics*, vol. 54, no. 6, pp. 3255–3259, 1983.

[146] K. Kudo, M. Yamashina, and T. Moriizumi, "Field effect measurement of organic dye films," *Japanese Journal of Applied Physics*, vol. 23, no. 1, pp. 130–130, 1984.

[147] A. Tsumura, H. Koezuka, and T. Ando, "Macromolecular electronic device: field-effect transistor with a polythiophene thin film," *Applied Physics Letters*, vol. 49, no. 18, pp. 1210–1212, 1986.

[148] W.-Y. Chou, S.-T. Lin, H.-L. Cheng et al., "Polymer light-emitting diodes with thermal inkjet printed poly(3,4-ethylenedioxythiophene):polystyrenesulfonate as transparent anode," *Thin Solid Films*, vol. 515, no. 7-8, pp. 3718–3723, 2007.

[149] D.-H. Lee, J. S. Choi, H. Chae, C.-H. Chung, and S. M. Cho, "Screen-printed white OLED based on polystyrene as a host polymer," *Current Applied Physics*, vol. 9, no. 1, pp. 161–164, 2009.

[150] A. Takakuwa, M. Misaki, Y. Yoshida, and K. Yase, "Micropatterning of emitting layers by microcontact printing and application to organic light-emitting diodes," *Thin Solid Films*, vol. 518, no. 2, pp. 555–558, 2009.

[151] S. Logothetidis, "Flexible organic electronic devices: materials, process and applications," *Materials Science and Engineering B: Solid-State Materials for Advanced Technology*, vol. 152, no. 1–3, pp. 96–104, 2008.

[152] Z. Bao and J. Locklin, Eds., *Organic Field-Effect Transistors*, CRC Press, 2007.

[153] P. Gomez-Romero and C. Sanchez, Eds., *Functional Hybrid Materials*, Wiley-VCH, 2004.

[154] C. W. Tang and S. A. vanslyke, "Organic electroluminescent diodes," *Applied Physics Letters*, vol. 51, no. 12, pp. 913–915, 1987.

[155] S. R. Forrest, "The path to ubiquitous and low-cost organic electronic appliances on plastic," *Nature*, vol. 428, no. 6986, pp. 911–918, 2004.

[156] S. Dasgupta, G. Stoesser, N. Schweikert et al., "Printed and electrochemically gated, high-mobility, inorganic oxide nanoparticle FETs and their suitability for high-frequency applications," *Advanced Functional Materials*, vol. 22, no. 23, pp. 4909–4919, 2012.

[157] M. Jørgensen, K. Norrman, S. A. Gevorgyan, T. Tromholt, B. Andreasen, and F. C. Krebs, "Stability of polymer solar cells," *Advanced Materials*, vol. 24, no. 5, pp. 580–612, 2012.

[158] A. Mishra and P. Bäuerle, "Small molecule organic semiconductors on the move: promises for future solar energy technology," *Angewandte Chemie: International Edition*, vol. 51, no. 9, pp. 2020–2067, 2012.

[159] X. Xu, M. Davanco, X. Qi, and S. R. Forrest, "Direct transfer patterning on three dimensionally deformed surfaces at micrometer resolutions and its application to hemispherical focal plane detector arrays," *Organic Electronics*, vol. 9, no. 6, pp. 1122–1127, 2008.

[160] R. Li, L. Jiang, Q. Meng et al., "Micrometer-sized organic single crystals, anisotropic transport, and field-effect transistors of a fused-ring thienoacene," *Advanced Materials*, vol. 21, no. 44, pp. 4492–4495, 2009.

[161] Y. Wu, P. Liu, B. S. Ong et al., "Controlled orientation of liquid-crystalline polythiophene semiconductors for high-performance organic thin-film transistors," *Applied Physics Letters*, vol. 86, no. 14, Article ID 142102, pp. 1–3, 2005.

[162] L. Li, Q. Tang, H. Li et al., "An ultra closely π-stacked organic semiconductor for high performance field-effect transistors," *Advanced Materials*, vol. 19, no. 18, pp. 2613–2617, 2007.

[163] T. Toccoli, M. Tonezzer, P. Bettotti et al., "Supersonic molecular beams deposition of α-quaterthiophene: Enhanced growth control and devices performances," *Organic Electronics*, vol. 10, no. 3, pp. 521–526, 2009.

[164] M. Tonezzer, E. Rigo, S. Gottardi et al., "Role of kinetic energy of impinging molecules in the α-sexithiophene growth," *Thin Solid Films*, vol. 519, no. 12, pp. 4110–4113, 2011.

[165] S. Gottardi, T. Toccoli, S. Iannotta et al., "Optimizing picene molecular assembling by supersonic molecular beam deposition," *Journal of Physical Chemistry C*, vol. 116, no. 46, pp. 24503–24511, 2012.

[166] H. Antoniadis, M. A. Abkowitz, and B. R. Hsieh, "Carrier deep-trapping mobility-lifetime products in poly(p-phenylene

vinylene)," *Applied Physics Letters*, vol. 65, no. 16, pp. 2030–2032, 1994.

[167] M. Chikamatsu, T. Mikami, J. Chisaka et al., "Ambipolar organic field-effect transistors based on a low band gap semiconductor with balanced hole and electron mobilities," *Applied Physics Letters*, vol. 91, no. 4, Article ID 043506, 2007.

[168] C.-Y. Yang, S.-S. Cheng, C.-W. Ou, Y.-C. Chuang, M.-C. Wu, and C.-W. Chu, "Balancing the ambipolar conduction for pentacene thin film transistors through bifunctional electrodes," *Applied Physics Letters*, vol. 92, no. 25, Article ID 253307, 2008.

[169] S. Reineke, F. Lindner, G. Schwartz et al., "White organic light-emitting diodes with fluorescent tube efficiency," *Nature*, vol. 459, no. 7244, pp. 234–238, 2009.

[170] R. Meerheim, M. Furno, S. Hofmann, B. Lüssem, and K. Leo, "Quantification of energy loss mechanisms in organic light-emitting diodes," *Applied Physics Letters*, vol. 97, no. 25, Article ID 253305, 2010.

[171] H. Sasabe, T. Chiba, S.-J. Su, Y.-J. Pu, K.-I. Nakayama, and J. Kido, "2-Phenylpyrimidine skeleton-based electron-transport materials for extremely efficient green organic light-emitting devices," *Chemical Communications*, no. 44, pp. 5821–5823, 2008.

[172] S.-J. Su, D. Tanaka, Y.-J. Li, H. Sasabe, T. Takeda, and J. Kido, "Novel four-pyridylbenzene-armed biphenyls as electron-transport materials for phosphorescent OLEDs," *Organic Letters*, vol. 10, no. 5, pp. 941–944, 2008.

[173] S.-J. Su, E. Gonmori, H. Sasabe, and J. Kido, "Highly efficient organic blue-and white-light-emitting devices having a carrier-And exciton-confining structure for reduced efficiency roll-off," *Advanced Materials*, vol. 20, no. 21, pp. 4189–4194, 2008.

[174] L. Xiao, S.-J. Su, Y. Agata, H. Lan, and J. Kido, "Nearly 100% internal quantum efficiency in an organic blue-light electrophosphorescent device using a weak electron transporting material with a wide energy gap," *Advanced Materials*, vol. 21, no. 12, pp. 1271–1274, 2009.

[175] F. Laquai, Y.-S. Park, J.-J. Kim, and T. Basché, "Excitation energy transfer in organic materials: From fundamentals to optoelectronic devices," *Macromolecular Rapid Communications*, vol. 30, no. 14, pp. 1203–1231, 2009.

[176] A. Köler and H. Bässler, "Triplet states in organic semiconductors," *Materials Science and Engineering R: Reports*, vol. 66, no. 4–6, pp. 71–109, 2009.

[177] S. Chénais and S. Forget, "Recent advances in solid-state organic lasers," *Polymer International*, vol. 61, no. 3, pp. 390–406, 2012.

[178] A. Buckley, Ed., *Organic Light Emitting Diodes*, Woodhead, 2013.

[179] D. Yan, H. Wang, and B. Du, *Introduction to Organic senicon-ductor Heterojunctions*, John Wiley & Sons, 2010.

[180] J. A. Rogers, Z. Bao, K. Baldwin et al., "Paper-like electronic displays: Large-area rubber-stamped plastic sheets of electronics and microencapsulated electrophoretic inks," *Proceedings of the National Academy of Sciences of the United States of America*, vol. 98, no. 9, pp. 4835–4840, 2001.

[181] C. D. Sheraw, L. Zhou, J. R. Huang et al., "Organic thin-film transistor-driven polymer-dispersed liquid crystal displays on flexible polymeric substrates," *Applied Physics Letters*, vol. 80, no. 6, pp. 1088–1090, 2002.

[182] H. Kawaguchi, T. Someya, T. Sekitani, and T. Sakurai, "Cut-and-paste customization of organic FET integrated circuit and its application to electronic artificial skin," *IEEE Journal of Solid-State Circuits*, vol. 40, no. 1, pp. 177–185, 2005.

[183] P. F. Baude, D. A. Ender, M. A. Haase, T. W. Kelley, D. V. Muyres, and S. D. Theiss, "Pentacene-based radio-frequency identification circuitry," *Applied Physics Letters*, vol. 82, no. 22, pp. 3964–3966, 2003.

[184] K. Myny, S. van Winckel, S. Steudel et al., "An inductively-coupled 64b organic RFID tag operating at 13.56MHz with a data rate of 787b/s," in *Proceedings of the IEEE International Solid State Circuits Conference (ISSCC '08)*, pp. 285–614, February 2008.

[185] Y. Ohmori, M. Hikita, H. Kajii et al., "Organic electroluminescent diodes as a light source for polymeric waveguides toward organic integrated optical devices," *Thin Solid Films*, vol. 393, no. 1-2, pp. 267–272, 2001.

[186] Y. Ohmori, H. Kajii, M. Kaneko et al., "Realization of polymeric optical integrated devices utilizing organic light-emitting diodes and photodetectors fabricated on a polymeric waveguide," *IEEE Journal on Selected Topics in Quantum Electronics*, vol. 10, no. 1, pp. 70–78, 2004.

[187] M. C. Gather, F. Ventsch, and K. Meerholz, "Embedding organic light-emitting diodes into channel waveguide structures," *Advanced Materials*, vol. 20, no. 10, pp. 1966–1971, 2008.

[188] M. C. Gwinner, S. Khodabakhsh, M. H. Song, H. Schweizer, H. Giessen, and H. Sirringhaus, "Integration of a rib waveguide distributed feedback structure into a light-emitting polymer field-effect transistor," *Advanced Functional Materials*, vol. 19, no. 9, pp. 1360–1370, 2009.

[189] S. Sakka, *Handbook of Sol-Gel Science and Technology*, Kluwer Academic, 2005.

[190] C. J. Brinker and G. W. Scherer, *Sol-Gel Science*, Academic Press, San Diego, Calif, USA, 1990.

[191] G. D. Sorarù, S. Modena, P. Bettotti, G. Das, G. Mariotto, and L. Pavesi, "Si nanocrystals obtained through polymer pyrolysis," *Applied Physics Letters*, vol. 83, no. 4, pp. 749–751, 2003.

[192] G. Das, L. Ferraioli, P. Bettotti et al., "Si-nanocrystals/SiO_2 thin films obtained by pyrolysis of sol-gel precursors," *Thin Solid Films*, vol. 516, no. 20, pp. 6804–6807, 2008.

[193] E. J. Henderson, J. A. Kelly, and J. G. C. Veinot, "Influence of $HSiO_{1.5}$ sol-gel polymer structure and composition on the size and luminescent properties of silicon nanocrystals," *Chemistry of Materials*, vol. 21, no. 22, pp. 5426–5434, 2009.

[194] A. Karakuscu, R. Guider, L. Pavesi, and G. D. Sorarù, "White luminescence from sol-gel-derived SiOC thin films," *Journal of the American Ceramic Society*, vol. 92, no. 12, pp. 2969–2974, 2009.

[195] C. Chen, C. Han, L. Wang et al., "650-nm all-polymer thermo-optic waveguide switch arrays based on novel organic-inorganic grafting PMMA materials," *IEEE Journal of Quantum Electronics*, vol. 49, no. 5, pp. 447–453, 2013.

[196] X. Zhang, M. Qian, X. Zeng, Z. Zhao, J. Lasante, and P. Plante, "Design and fabrication of single mode rib waveguides using sol-gel derived organic-inorganic hybrid materials," *Journal of Sol-Gel Science and Technology*, vol. 45, no. 1, pp. 103–107, 2008.

[197] C. Y. Jia, W. Que, and W. G. Liu, "Preparation and optical properties of sol-gel derived photo-patternable organic-inorganic hybrid films for optical waveguide applications," *Thin Solid Films*, vol. 518, no. 1, pp. 290–294, 2009.

[198] P. Karasiński, C. Tyszkiewicz, R. Rogoziński, and J. Jaglarz, "Optical rib waveguides based on sol-gel derived silica-titania films," *Thin Solid Films*, vol. 519, no. 16, pp. 5544–5551, 2011.

[199] S. Krivec, N. Matsko, V. Satzinger et al., "Silica-based, organically modified host material for waveguide structuring by two-photon-induced photopolymerization," *Advanced Functional Materials*, vol. 20, no. 5, pp. 811–819, 2010.

[200] X. Zhang, W. Que, J. Chen, T. Gao, J. Hu, and W. Liu, "Fabrication of ridge waveguide structure from photosensitive TiO 2/ormosil hybrid films by using an ultraviolet soft imprint technique," *Thin Solid Films*, vol. 531, pp. 119–124, 2013.

[201] R. A. S. Ferreira, P. S. André, and L. D. Carlos, "Organic-inorganic hybrid materials towards passive and active architectures for the next generation of optical networks," *Optical Materials*, vol. 32, no. 11, pp. 1397–1409, 2010.

[202] Y. Enami, C. T. Derose, D. Mathine et al., "Hybrid polymersol-gel waveguide modulators with exceptionally large electro-optic coefficients," *Nature Photonics*, vol. 1, no. 3, pp. 180–185, 2007.

[203] Y. Enami, D. Mathine, C. T. Derose et al., "Hybrid electro-optic polymer/sol-gel waveguide directional coupler switches," *Applied Physics Letters*, vol. 94, no. 21, Article ID 213513, 2009.

[204] D. Psaltis, S. R. Quake, and C. Yang, "Developing optofluidic technology through the fusion of microfluidics and optics," *Nature*, vol. 442, no. 7101, pp. 381–386, 2006.

[205] F. Intonti, S. Vignolini, V. Türck et al., "Rewritable photonic circuits," *Applied Physics Letters*, vol. 89, no. 21, Article ID 211117, 2006.

[206] S.-W. Hwang, H. Tao, D.-H. Kim et al., "A physically transient form of silicon electronics," *Science*, vol. 337, no. 6102, pp. 1640–1644, 2012.

[207] M. Irimia-Vladuab, "Green electronics: biodegradable and biocompatible materials and devices for sustainable future," *Chemical Society Review*, vol. 43, no. 2, pp. 588–610, 2014.

[208] H. Tao, M. A. Brenckle, M. Yang et al., "Silk-based conformal, adhesive, edible food sensors," *Advanced Materials*, vol. 24, no. 8, pp. 1067–1072, 2012.

[209] B. D. Lawrence, M. Cronin-Golomb, I. Georgakoudi, D. L. Kaplan, and F. G. Omenetto, "Bioactive silk protein biomaterial systems for optical devices," *Biomacromolecules*, vol. 9, no. 4, pp. 1214–1220, 2008.